

## **Copyright Warning & Restrictions**

The copyright law of the United States (Title 17, United States Code) governs the making of photocopies or other reproductions of copyrighted material.

Under certain conditions specified in the law, libraries and archives are authorized to furnish a photocopy or other reproduction. One of these specified conditions is that the photocopy or reproduction is not to be “used for any purpose other than private study, scholarship, or research.” If a user makes a request for, or later uses, a photocopy or reproduction for purposes in excess of “fair use” that user may be liable for copyright infringement,

This institution reserves the right to refuse to accept a copying order if, in its judgment, fulfillment of the order would involve violation of copyright law.

**Please Note: The author retains the copyright while the New Jersey Institute of Technology reserves the right to distribute this thesis or dissertation**

Printing note: If you do not wish to print this page, then select “Pages from: first page # to: last page #” on the print dialog screen

The Van Houten library has removed some of the personal information and all signatures from the approval page and biographical sketches of theses and dissertations in order to protect the identity of NJIT graduates and faculty.

## **ABSTRACT**

### **Computer Simulation of Intracranial Hemodynamics During the Induction Phase of Anesthesia**

by

**Gopinath P. Sundaram**

The induction of general anesthesia is associated with severe hemodynamic compromises which, in turn, may cause acute elevation of intracranial pressure (ICP). Quantitative assessment of cerebrovascular responses arising from multiple mechanical and pharmacological interventions occurring in a short time interval require a large number of human studies which are difficult to perform. The purpose of this project is to evaluate the effect of various stimuli on the intracranial hemodynamics during induction using a mathematical model of cerebrovascular circulation.

A five compartmental model of the cerebrovascular system is used for our simulation. Autoregulation is modeled by adjusting arterial-arteriolar resistance in order to change the flow towards its control value. The effect of thiopental on cerebrovascular circulation is simulated by a variable arteriolar resistance which is functionally dependent on the thiopental concentration. Thiopental concentration, in turn, is predicted by a three compartmental pharmacokinetic model. The simulation program was written in TUTSIM dynamic simulation language for an IBM compatible PC. The presented computer simulation permits development of an optimal drug administration schedule to control ICP during various phases of anesthesia. It was demonstrated that if the time interval between the administration of a drug and intubation is more than 2 minutes, an additional dose of thiopental is required to prevent elevation of ICP during laryngoscopy.

**Computer Simulation of Intracranial Hemodynamics During  
the Induction Phase of Anesthesia**

by

**Gopinath P. Sundaram**

A Thesis  
Submitted to the Faculty of  
New Jersey Institute of Technology  
in Partial Fulfillment of the Requirements for the Degree of  
Master of Science in Biomedical Engineering

Biomedical Engineering Committee

May 1993

Blank Page

## **BIOGRAPHICAL SKETCH**

**Author:** Gopinath P. Sundaram

**Degree:** Master of Science in Biomedical Engineering

**Date:** May 1993

**Date of Birth:**

**Place of Birth:**

**Undergraduate and Graduate Education:**

- Master of Science in Biomedical Engineering,  
New Jersey Institute of Technology, Newark, NJ, 1993
- Bachelor of Science in Electronics and Communication Engineering,  
Madurai Kamraj University, Madurai, India, 1990

**Presentations and Publications:**

Gopinath Sundaram, Dr. Bekker, Dr. Ritter, Dr. Kristol, "Computer Simulation of Intracranial Hemodynamics." 19th Northeast Bioengineering Conference, New Jersey Institute of Technology, Newark, New Jersey, 19 March 1993.

**This thesis is dedicated to my family**

## **ACKNOWLEDGMENT**

The author wishes to thank his thesis advisors, Dr. Arthur Ritter and Dr. Alex Bekker for patiently reviewing the progress of the thesis at every stage and helping him to plan it efficiently. This thesis would not have been successful but for their invaluable guidance and sincere concern.

Special thanks to Dr. Kristol for serving as a member of the committee.



## TABLE OF CONTENTS

Chapter	Page
1 INTRODUCTION . . . . .	1
1.1 Goals of the Present Study . . . . .	2
1.2 Review of Models . . . . .	3
1.3 TUTSIM . . . . .	7
2 MODEL DEVELOPMENT . . . . .	9
2.1 Cerebrovascular System Model . . . . .	9
2.1.1 Autoregulation . . . . .	12
2.1.2 Equations of the System . . . . .	14
2.1.3 Calculation of CBF . . . . .	16
2.1.4 Implementation in TUTSIM . . . . .	16
2.1.5 Validation of the Model . . . . .	19
2.2 Pharmacokinetics of Thiopental . . . . .	25
2.2.1 Model Equations . . . . .	27
2.2.2 Effect of Thiopental on MAP . . . . .	30
2.2.3 Effect of Thiopental on Arterial Resistance . . . . .	30
2.2.4 TUTSIM Implementation . . . . .	31
2.3 Induction . . . . .	35
3 RESULTS . . . . .	36
3.1 Simulation of Induction Processes . . . . .	36
4 DISCUSSION . . . . .	50
4.1 Assumptions . . . . .	51
4.2 Critique . . . . .	51
4.3 Interpretation . . . . .	52
4.4 Conclusion . . . . .	53
5 APPENDIX . . . . .	54
6 REFERENCES . . . . .	61

## LIST OF TABLES

<b>Table</b>	<b>Page</b>
1 Rate Constants Associated with Thiopental Pharmacokinetics . . . . .	27
2 MAP at Different Thiopental Concentrations and Time . . . . .	30

## LIST OF FIGURES

Figure	Page
2.1 Electrical Analog of the Cerebrovascular System . . . . .	10
2.2 Block Diagram of the Cerebrovascular System. . . . .	10
2.3 Tutsim Block Diagram of the Cerebrovascular System . . . . .	17
2.4 Autoregulation . . . . .	18
2.5a CBF at Different MAP . . . . .	21
2.5b CBF vs MAP . . . . .	22
2.6a ICP at Different MAP . . . . .	23
2.6b ICP vs MAP . . . . .	24
2.7 Thiopental Pharmacokinetics . . . . .	26
2.8 Thiopental Conc. in the Body . . . . .	28
2.9 Implementation of Thiopental Pharmacokinetics . . . . .	32
2.10 Effect of Thiopental on MAP . . . . .	33
2.11 Effect of Thiopental on Arterial Resistance . . . . .	33
2.12 Interrelationship Between Thiopental Pharmacokinetics and Cerebrovascular System. . . . .	34
3.1 ICP vs Time, Initial ICP=9.7mmHg . . . . .	38
3.2 ICP vs Time, Initial ICP=24mmHg . . . . .	39
3.3 ICP vs Time, Initial ICP=32mmHg . . . . .	40
3.4 ICP vs Time, Initial ICP=40mmHg . . . . .	41
3.5 ICP vs Time, Initial ICP=50mmHg . . . . .	42
3.6 ICP vs Time, Initial ICP=9.7mmHg . . . . .	43
3.7 ICP vs Time, Initial ICP=24mmHg . . . . .	44
3.8 ICP vs Time, Initial ICP=32mmHg . . . . .	45
3.9 ICP vs Time, Initial ICP=40mmHg . . . . .	46
3.10 ICP vs Time, Initial ICP=50mmHg . . . . .	47
3.11 CBF vs Time, Single Dose . . . . .	48

<b>Figure</b>	<b>Page</b>
3.12 CBF vs Time, Double Dose. . . . .	49

# CHAPTER 1

## INTRODUCTION

General anesthesia can be defined as a state characterized by unconsciousness, analgesia and muscle relaxation adequate for the required surgical procedure. Multiple pharmacological and mechanical manipulations are required to achieve this state. These actions are associated with severe stresses on the circulatory, respiratory and central nervous systems, which, in certain circumstances, can be detrimental to the patient, especially those with neurosurgical problems. Patients with neurosurgical problems have increased intracranial pressure (ICP), caused by a tumor or other intracranial space-occupying lesion. This increased ICP may lead to transcompartmental herniation of brain tissue. An increase in ICP can reduce cerebral perfusion pressure which reduces the cerebral blood supply and hence the nourishment to the brain. The goal of the induction phase of anesthesia is to minimize the untoward effects of drugs while maintaining homeostasis.

The induction phase is defined as that phase of anesthesia which makes the patient unresponsive to surgical stimuli. This involves several pharmacological and mechanical manipulations associated with severe hemodynamic stresses. The different stages of induction are :

1. Positioning of the patient and pre-oxygenation.
2. Administration of a sedative - hypotonic drug. Example: thiopental.
3. Monitor and control - assist ventilation to keep alveolar ventilation at normal level.
4. Injection of neuromuscular relaxant.

5. Laryngoscopy and intubation - this process is associated with substantial increase in sympathetic outflow which causes the MAP to go up. This, in turn, causes ICP and CBF to go up as well. This increase can be partially compensated by administration of thiopental.

### **1.1 Goals of the Present Study**

- 1) Real time simulation of the induction process for normal patients and patients with increased ICP.
- 2) Development of optimal drug administration strategy to minimize hemodynamic instability and reduce ICP with the help of the simulated induction process.

To achieve our objectives, we have to

- 1) Model the hemodynamics of the cerebrovascular system , i.e. the pressure-volume relationship between the various compartments.
- 2) Develop a pharmacokinetic model for the concerned drugs. This would help in obtaining the concentration of the drug in the body as a function of time.
- 3) Combine the models to get the MAP as a function of drug concentration and time.

The approach is to use a mathematical model to simulate the induction process. In contrast to animal models used frequently in medicine, physical and mathematical models provide the possibility of easy manipulation of system parameters. Since the application of a physical model is often limited to a particular question and a change of its structure is practically impossible, mathematical models offer more flexibility in those cases where they can be used.

## 1.2 Review of Models

Soreh et. al (1) used a seven compartmental model to elucidate the dynamics of the cerebrovascular system. The model assumes constant resistance that relates fluid flux to pressure gradient, and compliance between compartments that relate fluid accumulation to rate of pressure change. The resistance and compliance are lumped in the boundary between the compartments. The mass balance for the  $n^{\text{th}}$  compartment is expressed as

$$\sum_m C_{nm} \frac{dP_{nm}}{dt} + \sum_m Z_{nm} P_{nm} = Q_n$$

The above equation reveals that if there are seven compartments, there would be seven equations to be solved using TUTSIM. The solution of these equations require numeral values for several parameters which are not available in the literature. Similar results can be obtained by selectively grouping certain compartments. More importantly, autoregulation is overlooked in this model and the arterial resistance and compliance are assumed to be constants. In reality, arterial resistance and compliance are functions of perfusion pressure and flow rate. It is autoregulation that helps to maintain the CBF constant over a wide range of arterial pressure (50-150mmHg). Autoregulation plays an important role upon the effects of drugs, and hence this model would have to be extensively modified for our study.

In the model presented by Barge et. al (2), the assumptions made are, that the vascular bed behaves as an elastic compartment (which implies that variation in its volume is proportional to ICP), cerebrospinal fluid is passively reabsorbed by CSF valves and; CSF is passively produced by the choroid plexus. The expression given for ICP is

$$P(t) = Ae^{-Bt} + Ce^{-Bt}$$

where  $A$ ,  $B$ ,  $C$  are parameters which depend upon arterial pressure (AP) and CBF.

As the expression reveals, the model becomes too cumbersome to study the effects of varying the AP or CSF pressure, since they are embedded in the parameters rather than being independent variables. The model deals with autoregulation partially in the sense that variation of arterial compliance is dealt with but that of arterial resistance is not. Also, the model does not provide means for studying the pressure changes in other regions of the system except the brain tissue compartment.

The model presented by Hofferberth et. al (3), derives an expression for CSF production and absorption per unit time using regression analysis. The parameters for the constants and the expression for cerebrospinal fluid (CSF) pressure were obtained from animal experiments. These expressions describe the dynamics of the cerebrovascular system which were then simulated on a computer using CSMP software. This model was able to simulate some normal and pathological characteristics of CSF dynamics. A relationship between secretion pressure, rate of absorption and resulting CSF pressure could be calculated from this model. Autoregulation of the system can be tested by observing the CSF pressure during an elevation of arterial pressure. However, in the model not all variables which influence the production, absorption and pressure of CBF were taken into account. Some of the variables not considered are brain volume, intracranial blood volume and the intracerebral pathways of the cerebral circulation. Another drawback of the model was that the parameters used in the model were estimated from different species. The implications are that the absolute values obtained may not be correct and that not all of the pathological conditions would have occurred in all species.

In the model presented by Oskar Hoffmann (4), mathematical model of



the isolated intracranial system is described which includes autoregulation of CBF using a variable cerebrovascular resistance. The model also contains control circuits to simulate the short term behavior of blood pressure regulation by the baroreceptor reflex. The intracranial space is modeled as a rigid container with four compartments interconnected by flow resistances. The autoregulating resistance is in between the arterial and venous vessels representing small arteries, arterioles and venules. The dynamic behavior of this resistance, ICP, AP, venous pressure (VP) and CSF volume are described by differential equations. The advantages of this model are that, it can be used for parameter estimation and simulation studies to investigate the system behavior under different conditions. However, due to the complex structure of the model, it is not possible to compare it with existing models. Hence modifying the model by adding subsystems becomes rather difficult. Also, the model maps only a limited segment of the real system onto appropriate mathematical equations. For example, metabolic and respiratory factors have been omitted. Autoregulation due to cerebral perfusion pressure is included but not its dependence on CBF. Without this, even though acceptable, the model is rather incomplete and does not suit our requirements.

An electrical circuit model of the cerebral circulation was presented by Takemae et. al (5). Changes of pulsatile waves of the ICP and the cerebral blood volume (CBV) with ICP increment were investigated. The distributed elements were lumped to simplify the model. The values of the circuit elements were evaluated using the analogy between hydrodynamic and electrical systems. The results of the modelling were applied to rheoencephalography (REG) using an electrical impedance method or noninvasive ICP monitoring. The major drawback of the model is that a separate resistor is used to deal with autoregulation instead of varying the arterial resistance. It is not clear that there

is any justification for this extra resistance. Myogenic and metabolic factors on which resistance depends, were not discussed. The model also does not provide any means for artificially injecting fluid into the system. This would have helped in studying certain abnormal conditions. Hence, even though this model comes closest to our requirements, it could not be used.

Shulman et. al(6) developed a mathematical model of the cerebrospinal fluid system to clarify the kinetics of ICP. To develop the model, an electrical analog was used to approximate the hydrodynamics of the CSF system. A general equation predicting the time course of pressure was derived in terms of four parameters- the intracranial compliance, dural sinus pressure, resistance to absorption, and CSF formation. The role of each parameter in governing the dynamic equilibrium of ICP was determined. From the analysis, dynamic tests were developed for rapid measurement of CSF formation resistance, absorption resistance and bulk intracranial compliance. A good feature of this model is that it accommodates methods for artificially injecting fluid into the system. Also this was one of the few models using non-linear equations to describe intracranial compliance, which was considered to be a variable. If the ICP is assumed constant, the equations become linear. However, the model did not allow the arterial resistance to be a variable parameter. This capability is essential for modeling autoregulation.

Giammarco et. al (7) in their paper, propose a mathematical model that describes the production and diffusion of vasoactive chemical factors involved in oxygen dependent cerebral blood flow. Our model does not include chemical factors which alter arteriolar resistance since those mechanisms are not very well understood in a quantitative way. In the future, we may be able to extend our model to include the effects of endothelial derived relaxing factor (EDRF), nitric

oxide (NO) and other chemical agents on cerebral vascular resistance.

### 1.3 TUTSIM

A high level language is devised to relieve the user from the details of programming, thus permitting the user to focus his attention on solving the problem. In the early 1960's, analog computers had their own simple way of doing just that. They were usually programmed from a block diagram sketch and a list of equations representing the system being modeled. The analog computer, by definition, "solved" a problem by substitution of functional electrical analog blocks for real functions. Thus the block diagram of the real system and the block diagram for wiring up the analog computer were pretty much the same diagram.

Soon digital computers outpaced analog computers in speed, accuracy and economy. However the high level languages they brought in were modeled more to the inner working of the computer than to the realities of the problems that needed solutions. Most simulation programs followed these techniques, and often wound up more incomprehensible to the practicing engineer, than the computer languages themselves.

TUTSIM has re-established the analog between the real world systems and the computer model language. It has the convenience of an analog computer and the speed and accuracy of the digital computer. Furthermore, interaction with the user, and convenience of the use are enhanced by the availability of TUTSIM on the popular microcomputers of today.

Real time behavior is usually represented by linear and nonlinear differential equations. The solutions of these equations are made possible only by "continuous simulation", which can be realized by using TUTSIM. These

solutions can describe the movements and energetics of all the complex physiologic systems.

The biggest advantage of using TUTSIM is that the user does not have to be concerned about computer algorithms. However, the user must be able to determine the applicable equations of the system under consideration. TUTSIM blocks represent mathematical operations. TUTSIM block diagrams may be written from the equations term by term, or sometimes by direct inspection of the real system.

The flow is simply:

Problem :--->Mathematical Model :---> Block Model : --->Results

Model parameters such as initial values of an integration are easily entered and changed. Results are usually time dependent values and are available in graphical display or numerical tables on the screen or as hard copy.

Non-linear, discontinuous, and special mathematical blocks increase the power of TUTSIM far beyond the analog computers. The core of TUTSIM is written in assembly language. This allows for the fastest possible program execution and thus achieve "continuous simulation" of real time systems.

## CHAPTER 2

### MODEL DEVELOPMENT

#### 2.1 Cerebrovascular System Model

A modified version of the computer model of intracranial hemodynamics originally proposed by Mauro Ursino (8) is used for our simulation. The electrical analog of the system is shown in fig 2.1 and its equivalent compartmental representation is shown in fig 2.2. The system is considered to be a closed rigid system which cannot expand or contract. It is a multicompartmental system of constant total volume. This implies that if there is change in volume in any one compartment, it is compensated for by changes in volume in other compartments. As shown in fig 2.2, the different compartments are intracranial arterial vascular compartment, intracranial capillary compartment, the venous vascular compartment, venous sinus compartment and the brain tissue compartment. The input to the system is to the arterial vascular compartment and the outflow is from the venous sinus region. The 'openings' between adjacent compartments indicate that there is flow between them in the direction indicated by the arrow. The associated resistance is also indicated.

In the flow circuit,  $P_a$  is the arterial pressure which is the input to the system.  $R_{ai}$  is the arterial resistance. It is a variable resistor, i.e. it is 'autoregulated' in such a way that the intracranial pressure remains nearly constant over a wide range of arterial pressure.  $C_{ai}$  is the arterial compliance. It is a variable parameter and is a function of the difference between the arterial pressure and intracranial pressure. Mathematically it is expressed as

$$C_{ai} = \frac{dV_a}{d(P_a - P_{ic})} = \frac{1}{K_a (P_a - P_{ic})}$$

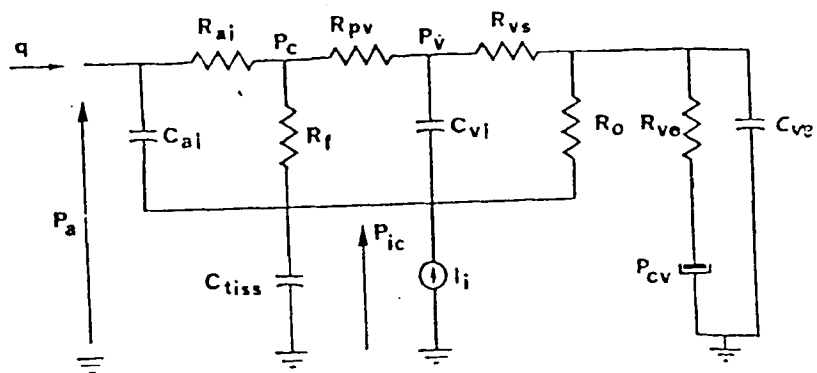


Fig. 2.1 Electrical Analog of the Cerebrovascular System

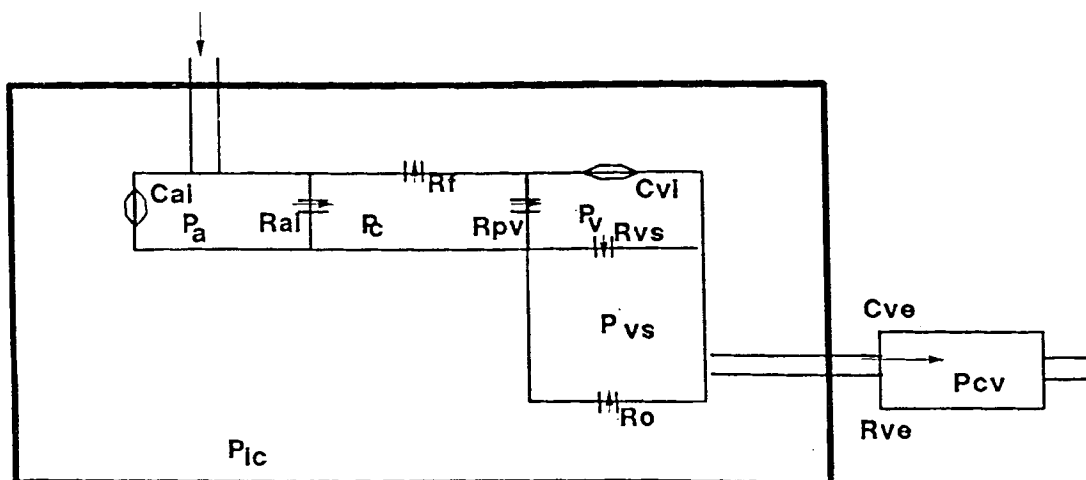


Fig. 2.2 Block Diagram of the Cerebrovascular System

where  $K_a$  is the elastance coefficient with units  $\text{cm}^{-3}$ .

$R_{pv}$  and  $R_{vs}$  are the resistance of the proximal venous vascular bed and resistance of the distal venous sinuses respectively. They are constants.  $R_f$  and  $R_o$  are the resistance to the formation and absorbance of cerebrospinal fluid (CSF). CSF is mainly formed by the choroid plexi of the cerebral ventricles and is mainly resorbed by the arachnoid villi of the dural sinuses. It is assumed in this model that CSF formation rate ( $q_f$ ) is proportional to the transmural pressure at the choroid capillary level ; i.e.

$$q_f = \frac{P_c - P_{ic}}{R_f}$$

The absorption of the CSF has been characterized by the following relation

$$q_a = \frac{P_{ic} - P_{vs}}{R_o}$$

where  $P_{vs}$  is the venous sinus pressure.

The compliance of the tissue region is represented by  $C_{tiss}$ . It is also a variable parameter and the following expression has been adopted for it.

$$1/C_{tiss} = -dP_{ic}/dV_{tiss} = K_e [P_{ic} + (P_{ic}/P_{01})^2]$$

where  $K_e$  and  $P_{01}$  are constant parameters. If ICP is low, the quadratic term in the above expression is negligible and the dependence of tissue elastance on pressure is fairly linear. However, when ICP rises, the quadratic term becomes relevant, which is reflected in a steeper increase in tissue elastance, the reciprocal of compliance.

$I_1$  in the circuit provides a way of infusing fluid artificially into the system. At normal conditions it is zero. This is helpful in studying the effects on

intracranial pressure if the volume of fluid increases by some pathological mechanism such as head trauma.

### **2.1.1 Autoregulation**

The arterial resistance ( $R_{ai}$ ) is autoregulated. Autoregulation of cerebral blood flow is a well documented phenomenon. Cerebral autoregulation is classically defined as the ability of the brain to maintain blood flow relatively constant over a wide range of perfusion pressures. This requires that cerebral vessels have the capability to constrict and dilate in response to an increased or decreased perfusion pressure respectively. Autoregulation is heterogeneous in several ways: regional, segmental and temporal. Regional heterogeneity of autoregulation is found during acute reductions and increases in systemic arterial pressure. Changes in blood flow are less in the brain stem than in cerebrum during decrease and increase in cerebral perfusion pressure. This finding suggests that the brain stem may be protected more effectively than the cerebrum from reduced delivery of substrate during hypotension, and from disruption of the blood-brain barrier during hypertension.

**Segmental heterogeneity:** A generally accepted concept is that arterioles are the major determinants of vascular resistance. However, in the cerebral circulation large arteries also contribute importantly to vascular resistance. Under control conditions arteries larger than 100-200  $\mu\text{m}$  in diameter account for 40-50 % of total cerebral vascular resistance. Kontos et al. (12) have systematically examined changes in diameter of pial arteries and arterioles during acute changes in arterial pressure. During reductions in pressure, the diameters of small arterioles (45 $\mu\text{m}$ ) became progressively greater as pressure was lowered below 80 mm Hg, but arteries 340 $\mu\text{m}$  in diameter dilated little below a mean arterial pressure of 100 mm Hg. In contrast, during an increase in pressure above 100 mm Hg, autoregulation appeared to reside primarily in the large pial



arteries. Large arteries constricted about 18% with an increase in pressure from 100 to 160 mm Hg, whereas the diameter of small arterioles did not change. Thus, while both large and small pial arteries contribute to the autoregulatory response of cerebral blood vessels, the relative response of each segment appears to vary depending on the level of arterial pressure. The differences in autoregulatory responses of large and small cerebral vessels may be related to the differences in wall stress in large and small resistance vessels.

**Temporal heterogeneity:** In addition to regional and segmental differences, the autoregulatory response also depends on the rate of increase in arterial pressure. By continuously monitoring the velocity of cerebral blood flow, the time course of its autoregulation during acute, moderate increases in arterial pressure was examined. Two to four seconds after increasing arterial pressure from 95 to 130 mm Hg with aortic obstruction, the velocity of blood flow was increased 64% and cerebral blood flow was increased 48%. Within 60 sec however, both velocity and cerebral blood flow had returned to control levels, even though the increase in arterial pressure was maintained. Thus, while the autoregulatory response to acute hypertension is relatively rapid, there is significant delay between the onset of hypertension and completion of the autoregulatory response (11).

Going into the mathematical aspects of autoregulation, the value of  $R_{ai}$  changes due to adjustments in the caliber of cerebral arteries and arterioles. These adjustments maintain cerebral blood flow rather close to normal, despite changes in cerebral perfusion pressure, provided this does not exceed a lower and upper limit (about 60-70 and 130-140 mm Hg, respectively). This phenomenon has been simulated by making use of the following equations.

$$\frac{dx}{dt} = -\frac{1}{\tau} x + \frac{1}{\tau} \left[ \frac{(P_a - P_v) - (P_{an} - P_{vn})}{P_{an} - P_{vn}} \right]$$

$$G_{ai} = G_{ain} \left[ 1 - \frac{1}{\pi} \arctan(x \cdot \pi) \right]$$

where  $x$  is a smooth muscle activation factor. It was experimentally found to be dependent on perfusion pressure changes. This dependence is described by eqn(1). Its dynamics have been characterized by a single real pole, with time constant  $\tau$ . The subscript  $n$  denotes a quantity in the normal equilibrium condition, and the transcendental function  $(1/\pi)\arctan(x \cdot \pi)$  has been introduced so as to have lower and upper saturation levels. When changes in perfusion pressure are very small, the result is

$$G_{ai} = G_{ain} [1 - x]$$

that is, the percent changes in arterial conductance are equal to the percent changes in perfusion pressure. However when perfusion pressure exceeds the lower or upper limit of autoregulation,  $G_{ai}$  settles at a value 50% greater or less than normal, respectively.

### 2.1.2 Equations of the System

Going back to the electrical circuit, Kirchoff's current law is applied to nodes 1, 2 and 3 and the following equations are derived.

#### Node 1:

$$Q_f = \frac{P_c - P_{ic}}{R_f} = \frac{P_a - P_{ic}}{R_{ai}} - \frac{P_c - P_v}{R_{pv}}$$

solving for  $P_c$

$$P_C \left[ \frac{1}{R_f} + \frac{1}{R_{ai}} + \frac{1}{R_{pv}} \right] = \frac{P_{ic}}{R_f} + \frac{P_a}{R_{ai}} + \frac{P_v}{R_{pv}}$$

$$\Rightarrow P_C = \frac{P_{ic}/R_f + P_a/R_{ai} + P_v/R_{pv}}{G_f + G_{ai} + G_{pv}} \quad (1)$$

**Node 2:**

$$C_{vi} \frac{d(P_v - P_{ic})}{dt} = \frac{P_C - P_v}{R_{pv}} + \frac{P_v - P_{vs}}{R_{vs}}$$

solving for  $P_v$

$$C_{vi} \frac{dP_v}{dt} = \frac{P_C}{R_{pv}} + \frac{P_{vs}}{R_{vs}} - P_v \left[ \frac{1}{R_{pv}} + \frac{1}{R_{vs}} \right] + C_{vi} \frac{dP_{ic}}{dt}$$

**Node 3:**

$$q_a = \frac{P_{ic} - P_{vs}}{R_o} = \frac{P_{vs} - P_{cv}}{R_{ve}} + \frac{P_v - P_{vs}}{R_{vs}} + C_{ve} \frac{dP_{vs}}{dt}$$

solving for  $P_{vs}$ ,

$$C_{ve} \frac{dP_{vs}}{dt} = \frac{P_{ic}}{R_o} + \frac{P_{cv}}{R_{ve}} - P_{vs} \left[ \frac{1}{R_o} + \frac{1}{R_{ve}} + \frac{1}{R_{vs}} \right] + \frac{P_v}{R_{vs}}$$

**Node 4:**

$$\frac{dV_a}{dt} + \frac{dV_v}{dt} + Q_f - Q_a + I_i = \frac{dV_{tiss}}{dt}$$

$$\Rightarrow C_{ai} \frac{d(P_a - P_{ic})}{dt} + C_{vi} \frac{d(P_v - P_{ic})}{dt} + \frac{P_c - P_{ic}}{R_{pv}} + \frac{P_{ic} - P_{vs}}{R_{vs}} + I_i$$

$$= C_{tiss} \frac{d P_{ic}}{dt}$$

The four equations, thus obtained, are solved using the simulation package TUTSIM. Here the input to the system is the mean arterial pressure ( $P_a$ , MAP). The outputs are the intracranial pressure ( $P_{ic}$ ), intracranial venous pressure ( $P_v$ ), intracranial capillary pressure ( $P_c$ ) and the venous sinus pressure ( $P_{vs}$ ). These pressures can be simulated for various values of  $P_a$ , abnormal and initial conditions.

**2.1.3 Calculation of CBF**

Cerebral blood flow depends on the pressure difference between the arterial pressure and the venous sinus pressure, and the overall resistance of the system. The overall resistance is calculated from the electrical circuit of the system. Now, the pressure difference is divided by the equivalent resistance to obtain cerebral blood flow in  $\text{cm}^3/\text{sec}$ .

**2.1.4 Implementation in TUTSIM**

The cerebrovascular system model thus developed is implemented in TUTSIM as shown in fig 2.3. Input to the system is arterial pressure ( $P_a$ ), which is the output of block 800. As it would be seen later, arterial pressure is a function of thiopental concentration in the body, and hence the input to the system is a

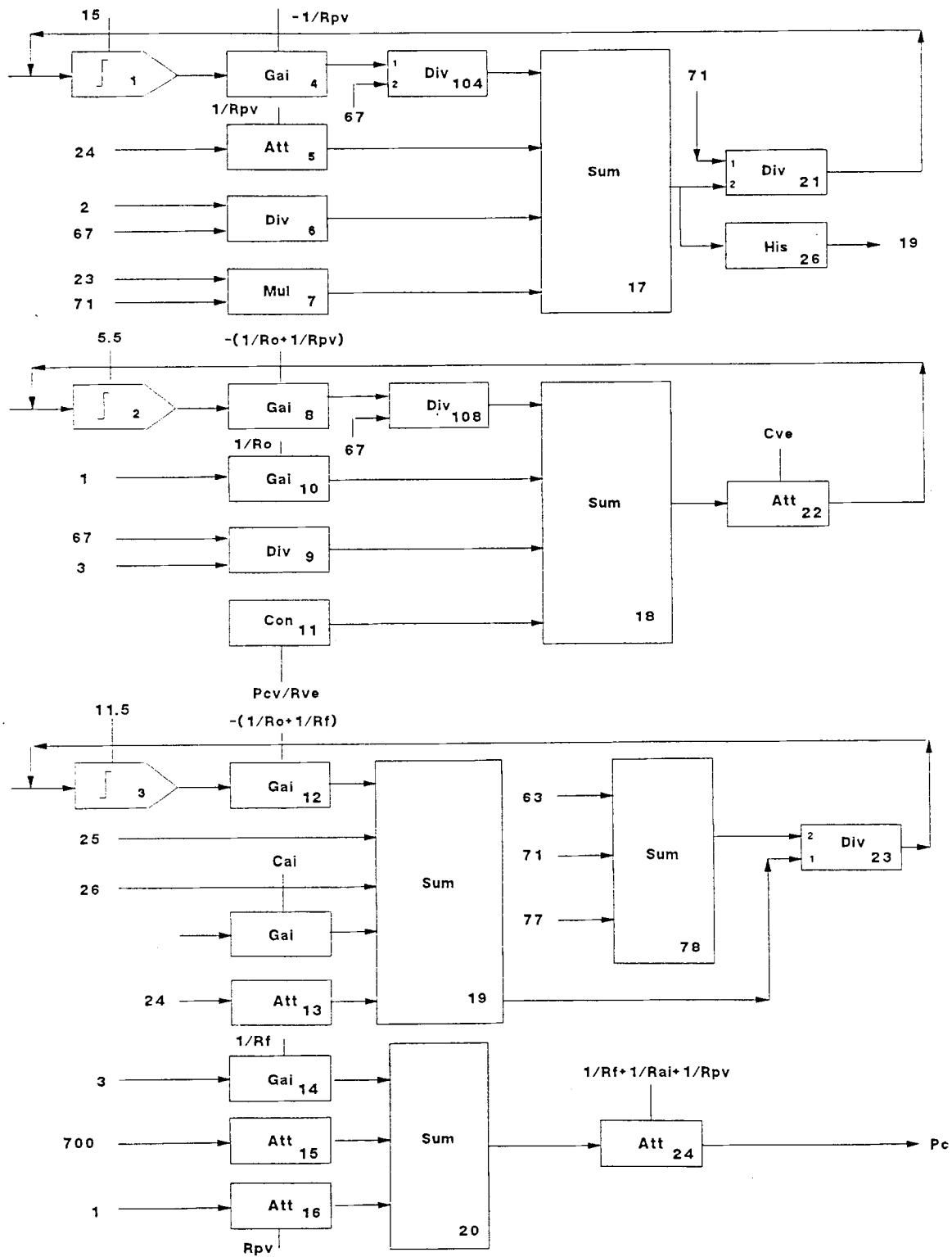


Fig. 2.3 TutSim Block Diagram of the Cerebrovascular System

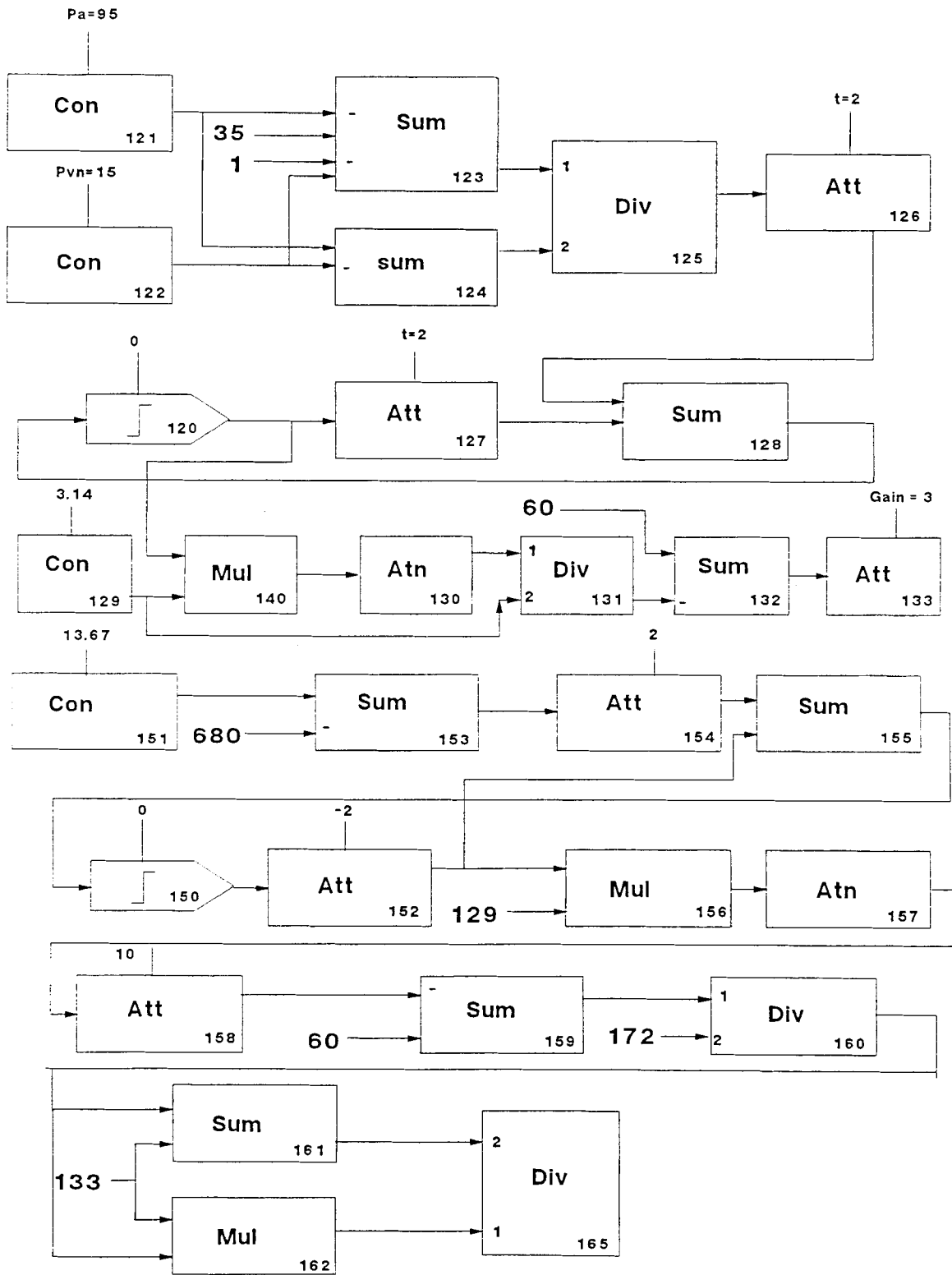


Fig. 2.4 Autoregulation

variable depending on thiopental concentration. The normal value of  $P_a$ , which is 95 mm Hg, is the parameter to the constant block 698. Hence under normal conditions this is the input to the system. Equation 1 is solved in blocks 14, 15, 16, 20 and 24. The output of block 24(attenuator) gives  $P_c$ , the required result. The solution of the differential equation 2, to get  $P_v$ , is implemented in blocks 1, 4, 5, 6, 7, 17 and 21. The output of block 1 (integrator) gives  $P_v$ . The parameter to this block is the initial condition of  $P_v$  which is 15 mm Hg. Equation 4 is solved to get  $P_{ic}$ . It is solved using blocks 3, 12, 13, 11, 25, 255 . The output of integrator block 3 gives  $P_{ic}$ . Its initial value is the parameter to block 3. Blocks 2, 8, 9, 10, 11, 18 and 22 are used to solve equation 3 to get  $P_{vs}$ . The output of block 2, which is again an integrator is  $P_{vs}$ . Thus the system of equations, which constitutes the model, are solved using various TUTSIM blocks.

**Autoregulation** : Implementation of autoregulation is done in the blocks between 120 and 165. It is shown in fig 2.4. The expression for autoregulation, stated earlier, is solved in these blocks. Blocks 121 and 122 are constant blocks with parameters  $P_{an}$  (normal arterial pressure) and  $P_{vn}$ (normal venous pressure) respectively. The sum blocks 123 and 124 are used to evaluate the numerator and denominator of the equation. The parameter to the attenuator block 126 is the time constant  $\tau$ . Block 120 is the integrator block, the output of which gives the activation factor. The parameter to the att block 133 is the normal arterial resistance. The output of this block is the autoregulated arterial resistance. The functions of the other blocks are trivial and needs no explanation.

### 2.1.5 Validation of the Model

To validate our model, that is, to prove that autoregulation has been implemented successfully, the following simulations are performed.

1. ICP vs time for various arterial pressures.
2. CBF vs time for various arterial pressures.

If autoregulation exists, then these parameters should nearly remain constant within the autoregulating range since the cerebral arterial resistance undergoes changes to maintain these parameters constant. Fig 2.5 and 2.6 show the simulations. The figures suggest that the autoregulating range for this system is between 70 and 150 mm Hg, which is in close agreement with the theoretical range. Thus the validation of our model is established.



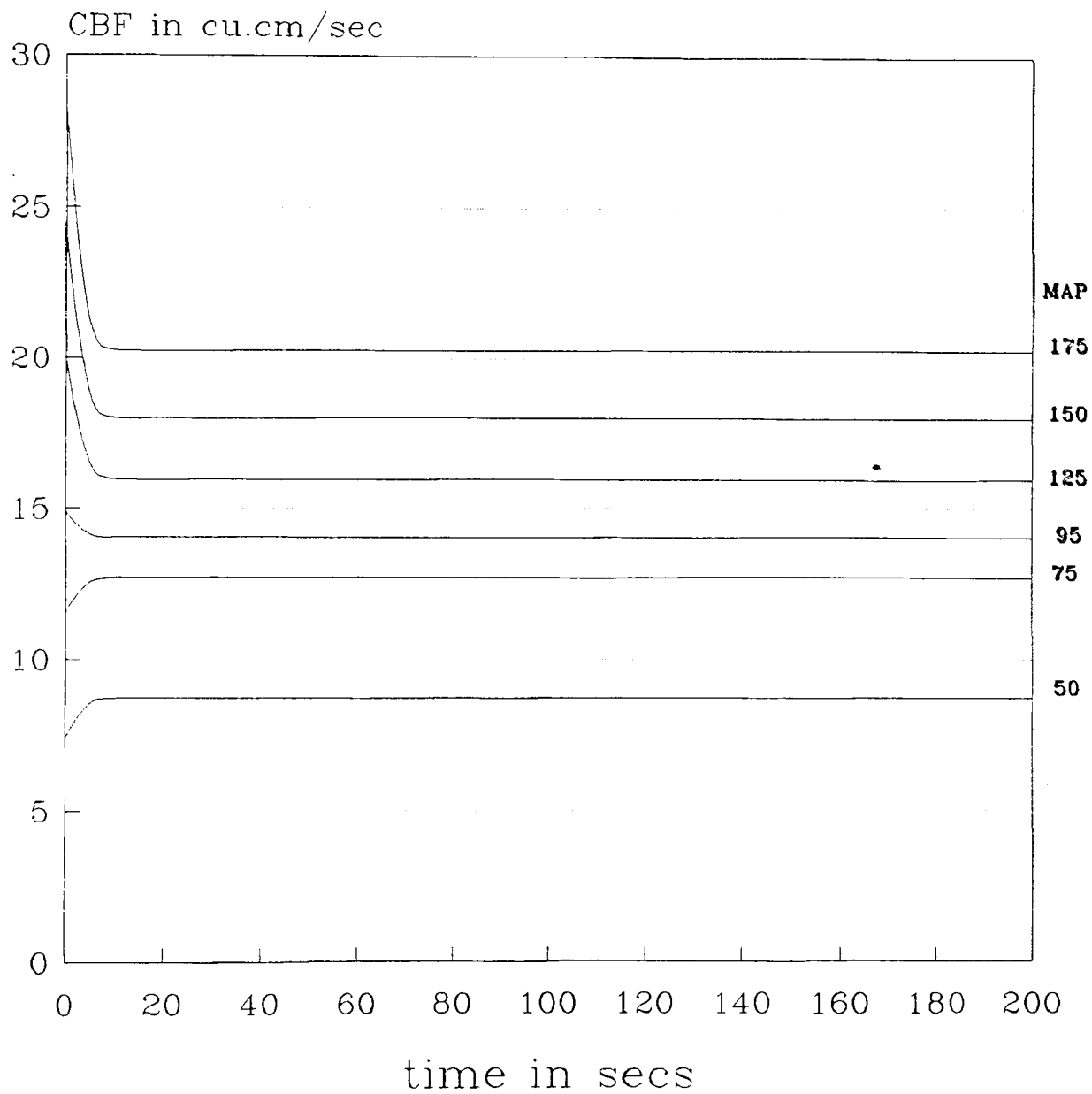


Fig. 2.5a CBF at Different MAP

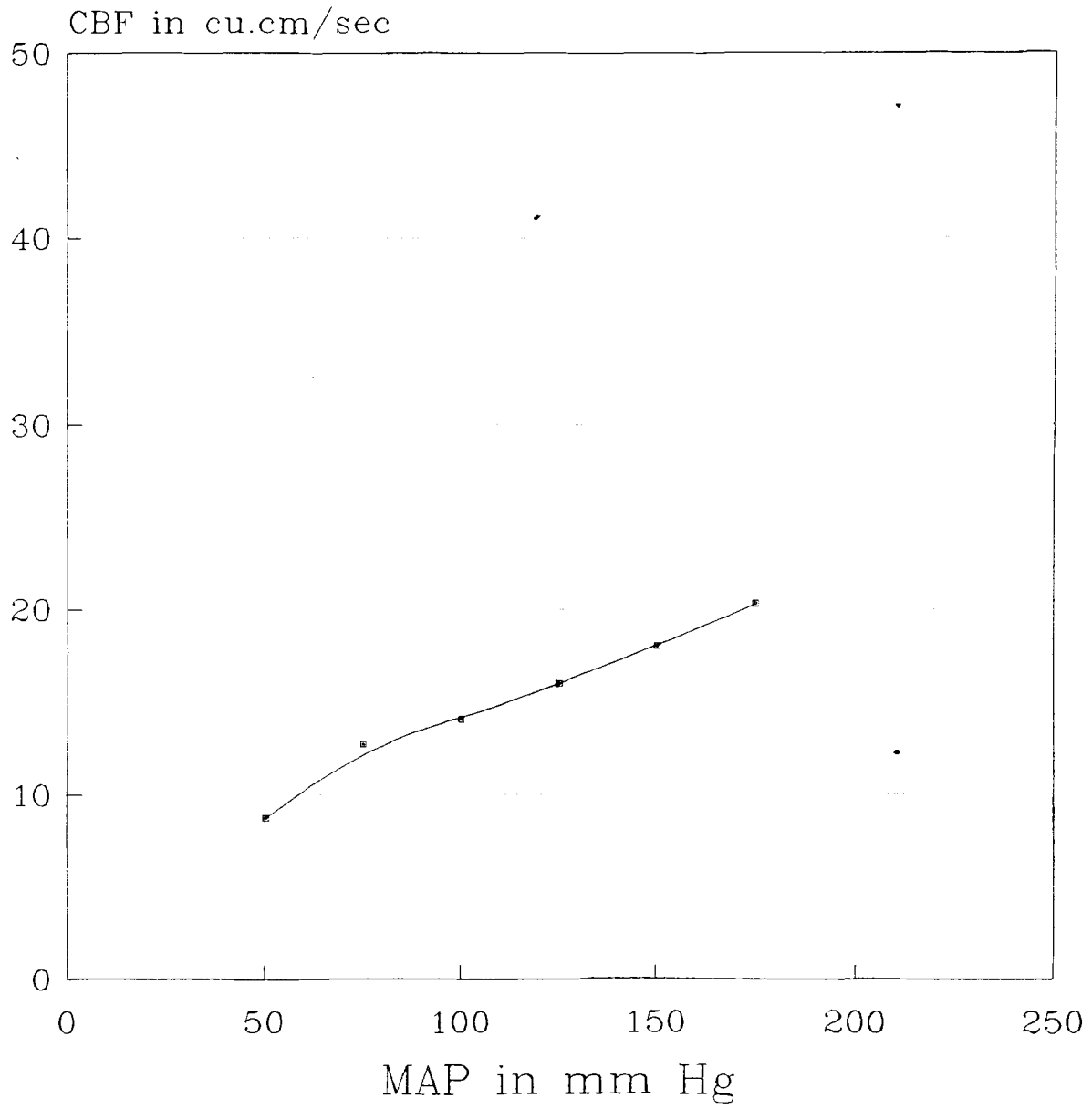


Fig. 2.5b CBF vs MAP

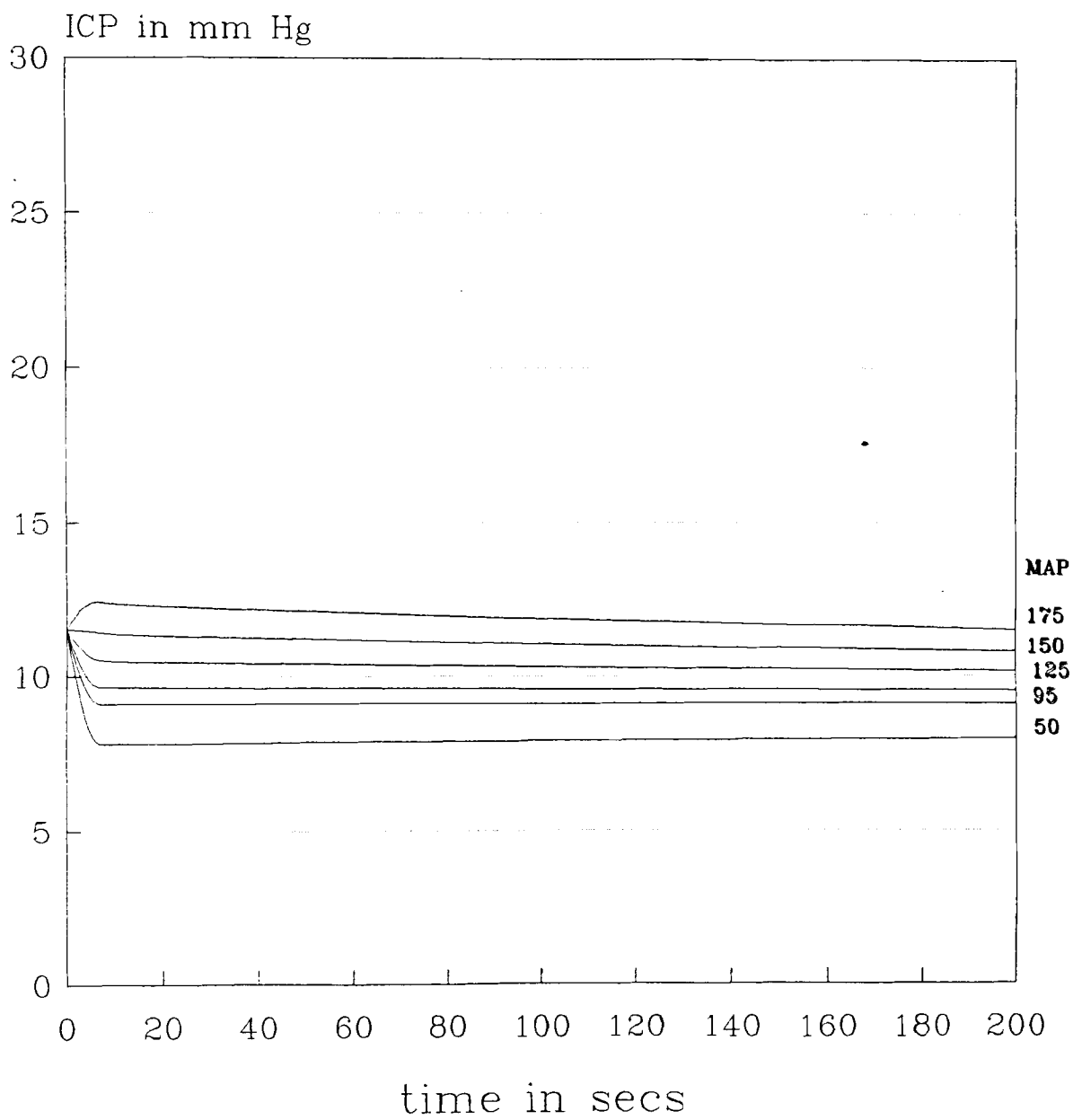


Fig. 2.6a ICP at Different MAP

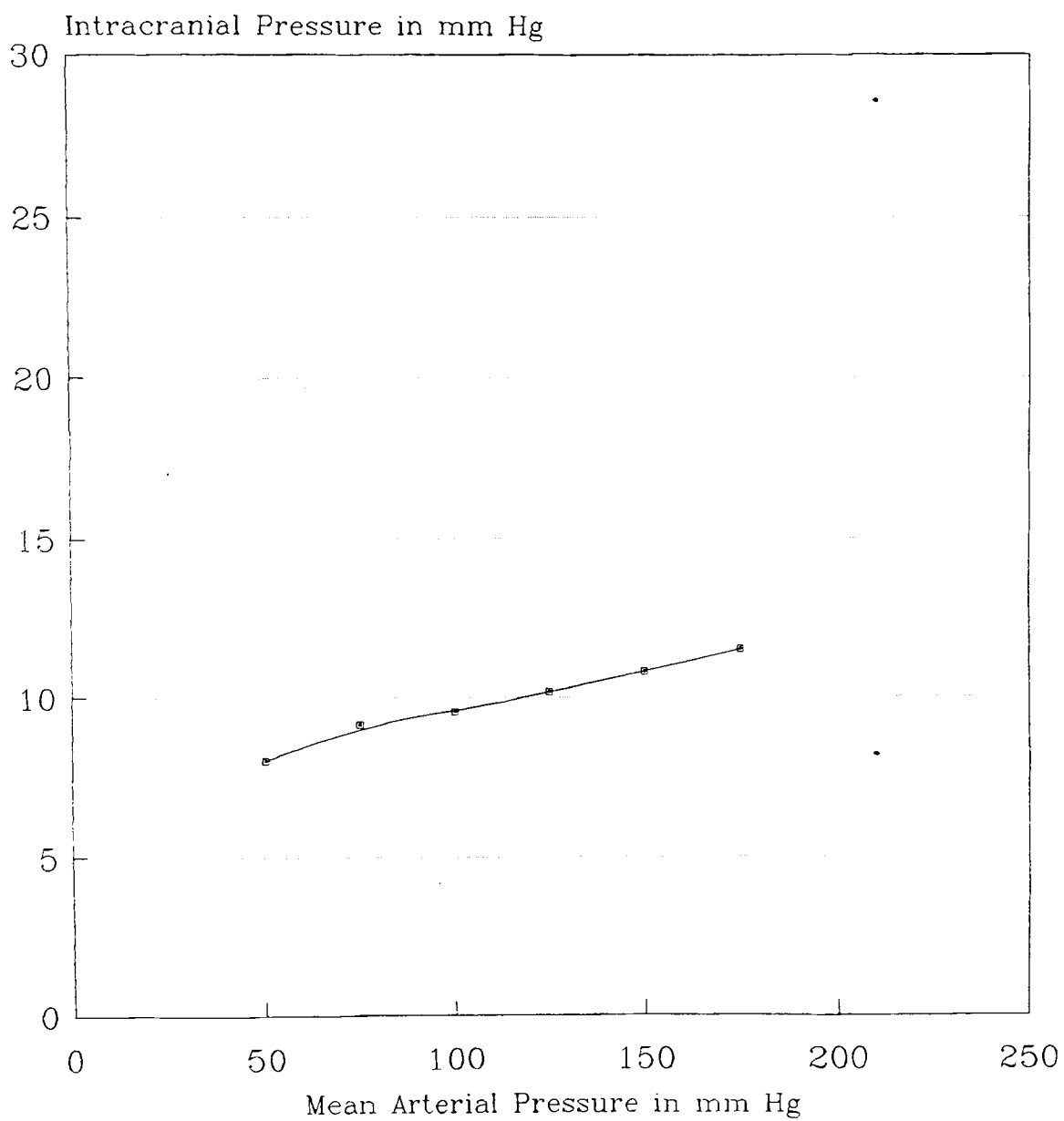


Fig. 2.6b ICP vs MAP

## 2.2 Pharmacokinetics of Thiopental

Barbiturates depress cerebral electrical activity and metabolism, and thus the need for oxygen delivery. This in turn leads to increased vascular resistance, decreased cerebral blood volume and decreased ICP. These are some of the requisites for a surgical process. Hence, thiopental being a barbiturate is the drug of choice for most neurosurgical patients.

In developing a pharmacokinetic model for thiopental distribution in the body, a three compartmental system is considered (13). According to this three compartmental open model, which is shown in fig 2.7, the drug is administered into a central compartment, followed by its distribution into two peripheral compartments, one of which is rapidly accessible, while the other is only slowly accessible. Elimination occurs only from the central compartment which contains the organs of metabolism and excretion. These compartments do not necessarily correspond to specific anatomical entities, although for many drugs the central compartment consists of the vascular space, with the richly perfused tissues such as the brain and the heart. The peripheral compartments are formed by less perfused tissues such as muscle, skin and fat. The distribution of thiopental to tissues is very rapid. The high lipid solubility of the drug is mainly responsible for this effect. The wide distribution of the drug is indicated by the apparent volume of distribution of the drug, the means of which vary between 1.5 and 2 times body weight.

The rate of transfer of drug from one compartment to another is associated with the rate constant,  $k$ . There are one or more rate constants associated with the transfer process. In general these rate processes are first order. The transfer of thiopental from the central and peripheral compartments is described by  $k_{12}$ ,  $k_{21}$ ,  $k_{13}$ ,  $k_{31}$  (fig 2.7). The mean ratio of  $k_{31}/k_{13}$  of .033

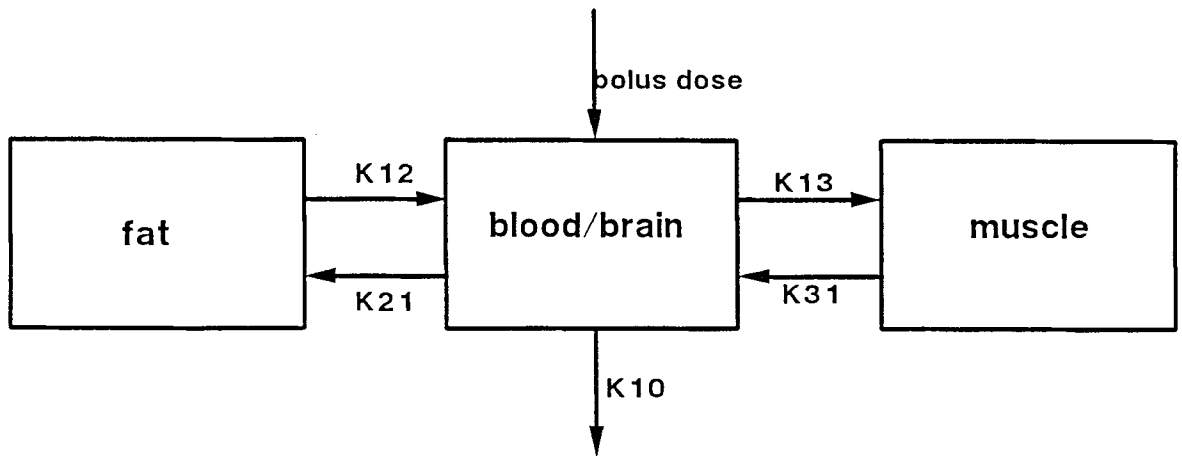


Fig. 2.7 Thiopental Pharmacokinetics

reflecting drug movement between the central and the deep peripheral compartment, suggests slow equilibrium between these compartments. On the other hand, the shallow compartment equilibrates more quickly, as reflected by two to three times greater ratios of  $k_{21}/k_{12}$ . The elimination rate constant  $k_{10}$  is, on the average, twice  $k_{31}$ , the rate of return of the drug from the deep peripheral compartment. Also only 9-15% of thiopental in the body is in the central compartment, available for elimination at any time. These findings suggest that the return of the drug to the central compartment from the deep peripheral compartment is rate-controlling in the elimination of thiopental. Table 1 shows the values of the rate constants for a normal person.

Table 1. Rate Constants Associated with Thiopental Pharmacokinetics

Rate Constants	in $10^{-5}/\text{sec}$
$k_{10}$	12.82
$k_{12}$	800
$k_{21}$	131.2
$k_{13}$	178.3
$k_{31}$	6.48

### 2.2.1 Model Equations

From the fig. 2.7, the mass balance equations for the three compartments are derived below. Let the mass in the body, fat and muscle compartments at any time  $t$  be  $B$ ,  $F$ ,  $M$  respectively. The rate of change of mass in any compartment is the difference between the rate of flow in and rate of flow out.

#### Body compartment:

$$\text{Flow in} = k_{12} \cdot F + k_{31} \cdot M$$

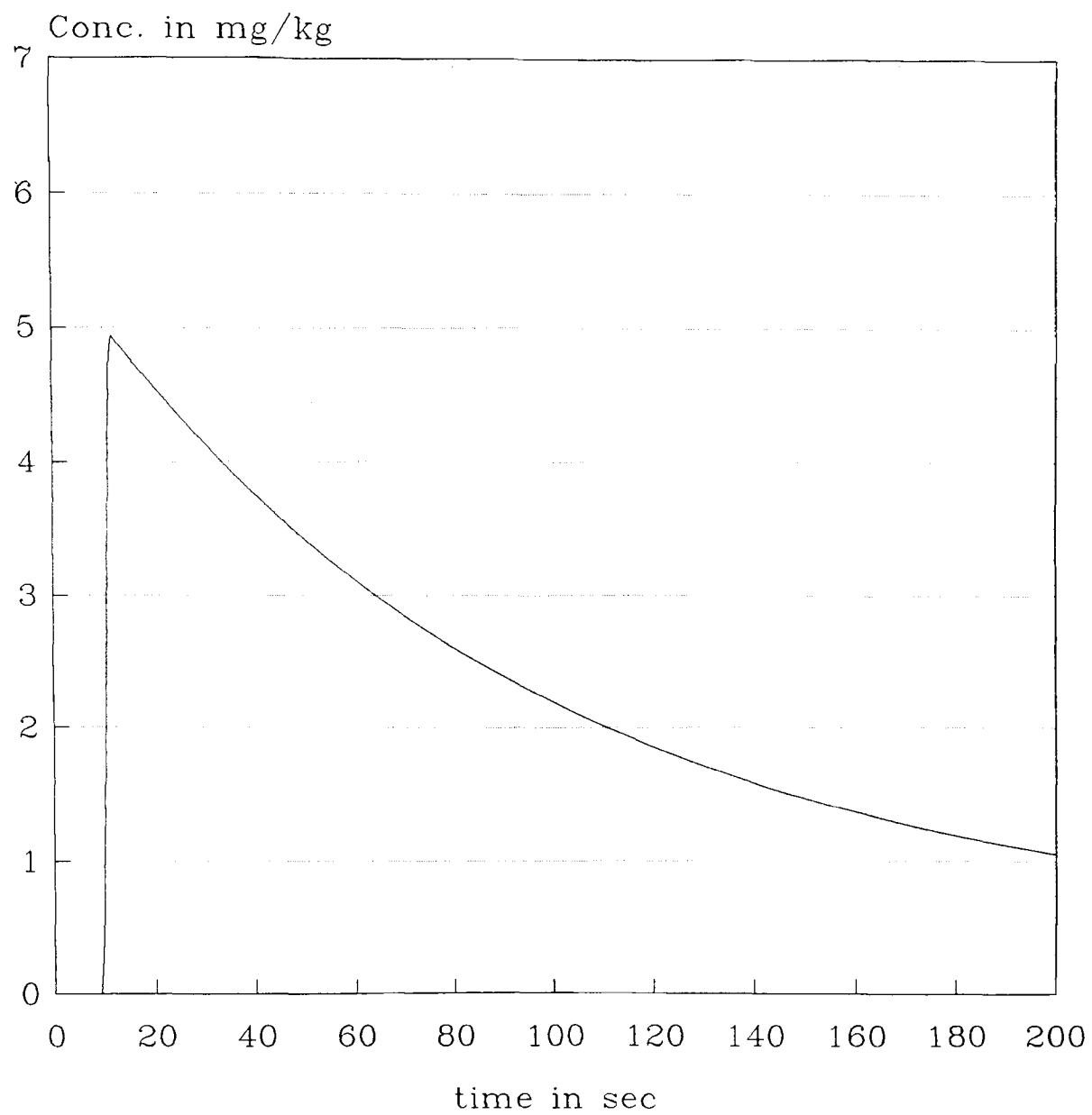


Fig. 2.8 Thiopental Conc. in the Body



$$\text{Flow out} = k_{21} \cdot B + k_{13} \cdot B + k_{10} \cdot B$$

$$\Rightarrow \frac{dB}{dt} = \text{Flow in} - \text{Flow out}$$

$$= k_{12} \cdot F + k_{31} \cdot M - k_{21} \cdot B - k_{13} \cdot B - k_{10} \cdot B$$

Initial Condition: At  $t = 0$ ,  $B = \text{bolus dose} = A \delta(t)$ .

**Fat compartment:**

$$\text{Flow in} = k_{21} \cdot B$$

$$\text{Flow out} = k_{12} \cdot F$$

$$\Rightarrow \frac{dF}{dt} = \text{Flow in} - \text{Flow out}$$

$$= k_{21} \cdot B - k_{12} \cdot F$$

Initial Condition: At  $t = 0$ ,  $F = 0$ .

**Muscle compartment:**

$$\text{Flow in} = k_{13} \cdot B$$

$$\text{Flow out} = k_{31} \cdot M$$

$$\Rightarrow \frac{dM}{dt} = k_{13} \cdot B - k_{31} \cdot M$$

Initial Condition: At  $t = 0$ ,  $M = 0$ .

These equations are solved using TUTSIM, and the concentration of thiopental with time in the body is simulated. The curve in fig 2.8 shows the simulation. It is a tri exponential curve.

Now the effects of thiopental on the mean arterial pressure and the arterial resistance must be developed to study the action of thiopental as a drug on the cerebrovasuclar system.

### 2.2.2 Effect of Thiopental on MAP

By giving a steady infusion of thiopental the variation of mean arterial pressure was studied(16). It was found that the mean arterial pressure decreased as the concentration of thiopental increased. Table 2 shows the MAP at different thiopental concentrations and time.

Table 2. MAP at Different Thiopental Concentrations and Time

Time in sec	Conc. of Thio	MAP
0	0	95.7
1	1	90.3
2	1.8	88.0
5	4.2	82.1

From the data in table 2, using line r regression, MAP as a function of thiopental concentration is given by the function

$$P_a = 95.15 - 3.32C$$

This function is now used as an input to the cerebrovascular system model.

### 2.2.3 Effect of Thiopental on Arterial Resistance

It was experimentally found that thiopental increases cerebral vascular resistance, decreases cerebral blood flow and the cerebral metabolic rate (14). However, the experimental results were qualitative rather than quantitative. To obtain quantitative results, the system which was developed so far was simulated for a given bolus dose of thiopental. Cerebral blood flow was plotted

as a function of time. The values obtained at different instants of time were compared with those obtained experimentally (17) to manipulate the changes in arterial resistance. It was assumed that the arterial resistance varies exponentially with the concentration according to the following relationship.

$$R_c = R_o(2 - e^{-x_c})$$

where  $R_c$  is the resistance, which varies dynamically with concentration,  $R_o$  is the normal value (at zero concentration), and  $x$  is the parameter to be determined.

It was found that CBF dropped to 50% of its normal value for a drug concentration of 30mg/kg. To get this effect in our simulation, the arterial resistance must be altered from 6 sec.mmHg/cm<sup>3</sup> to 9 sec.mmHg/cm<sup>3</sup>. Substituting these values in the equation above,  $x$  was found to be 0.366. Thus the effect of thiopental on arterial resistance was simulated.

Having incorporated the effects of thiopental on the MAP and arterial resistance, the model is now ready to simulate the actions of thiopental, as a drug on the system as a whole.

#### **2.2.4 TUTSIM Implementation**

The TUTSIM block diagram to simulate the thiopental pharmacokinetics is shown in fig 2.9. Output of integrator blocks 684, 685 and 686 give the concentration of thiopental in body, fat and muscle compartments respectively. The gain blocks 687-693 are used in the evaluation of  $dB/dt$ ,  $dF/dt$  and  $dM/dt$  with the relevant rate constants as their parameters. The sum blocks are used for the same purpose. The output of block 684(thiopental concentration in body) is

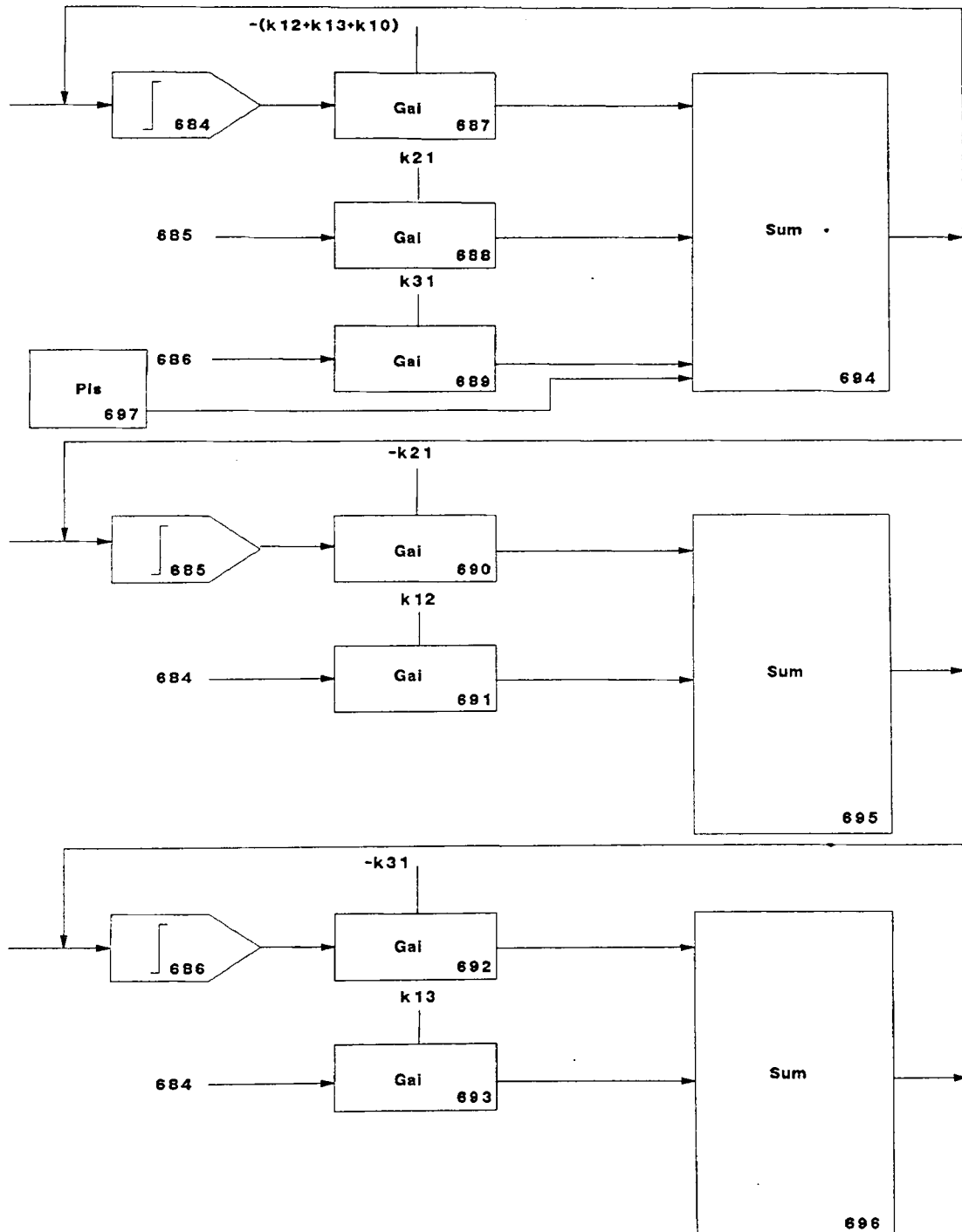


Fig. 2.9 Implementation of Thiopental Pharmacokinetics

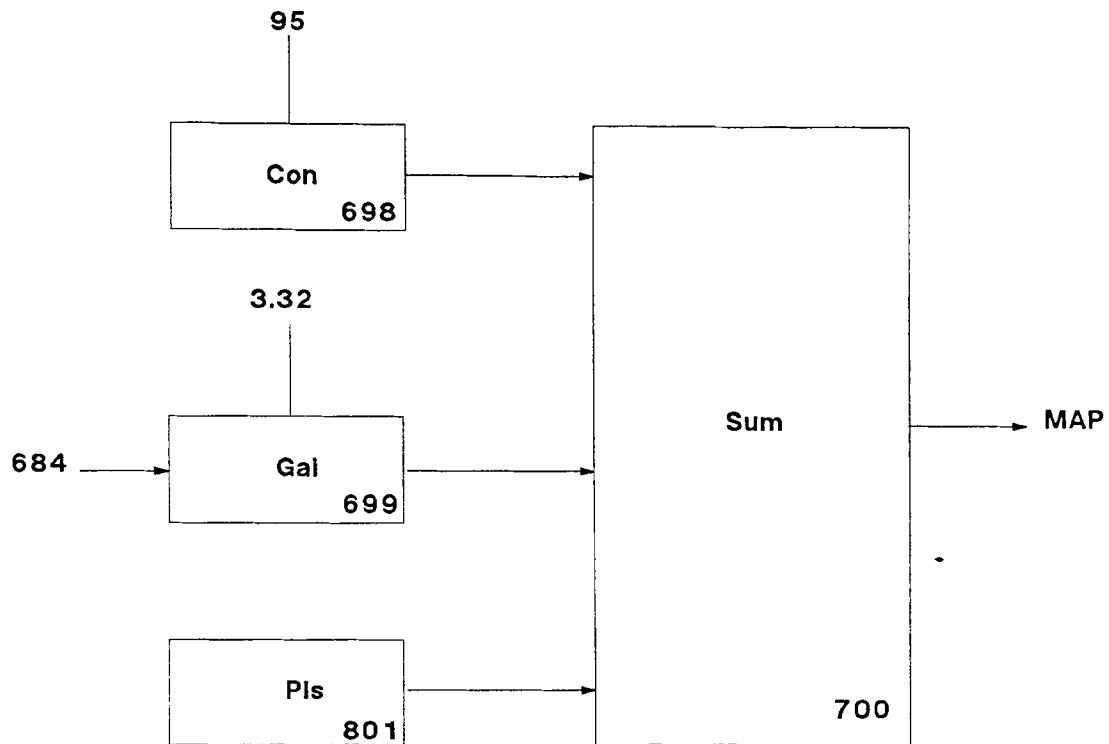


Fig. 2.10 Effect of Thiopental on MAP

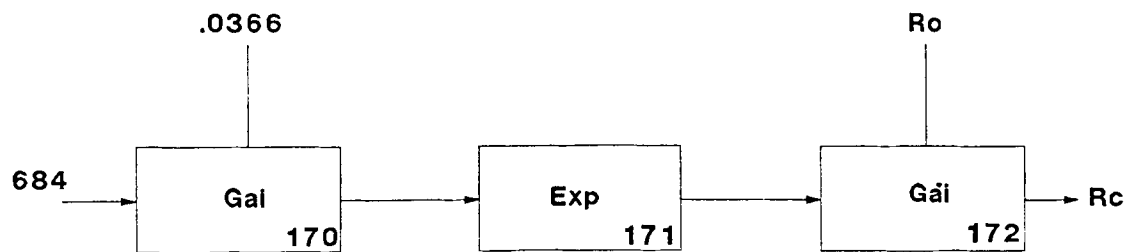


Fig. 2.11 Effect of Thiopental on Arterial Resistance

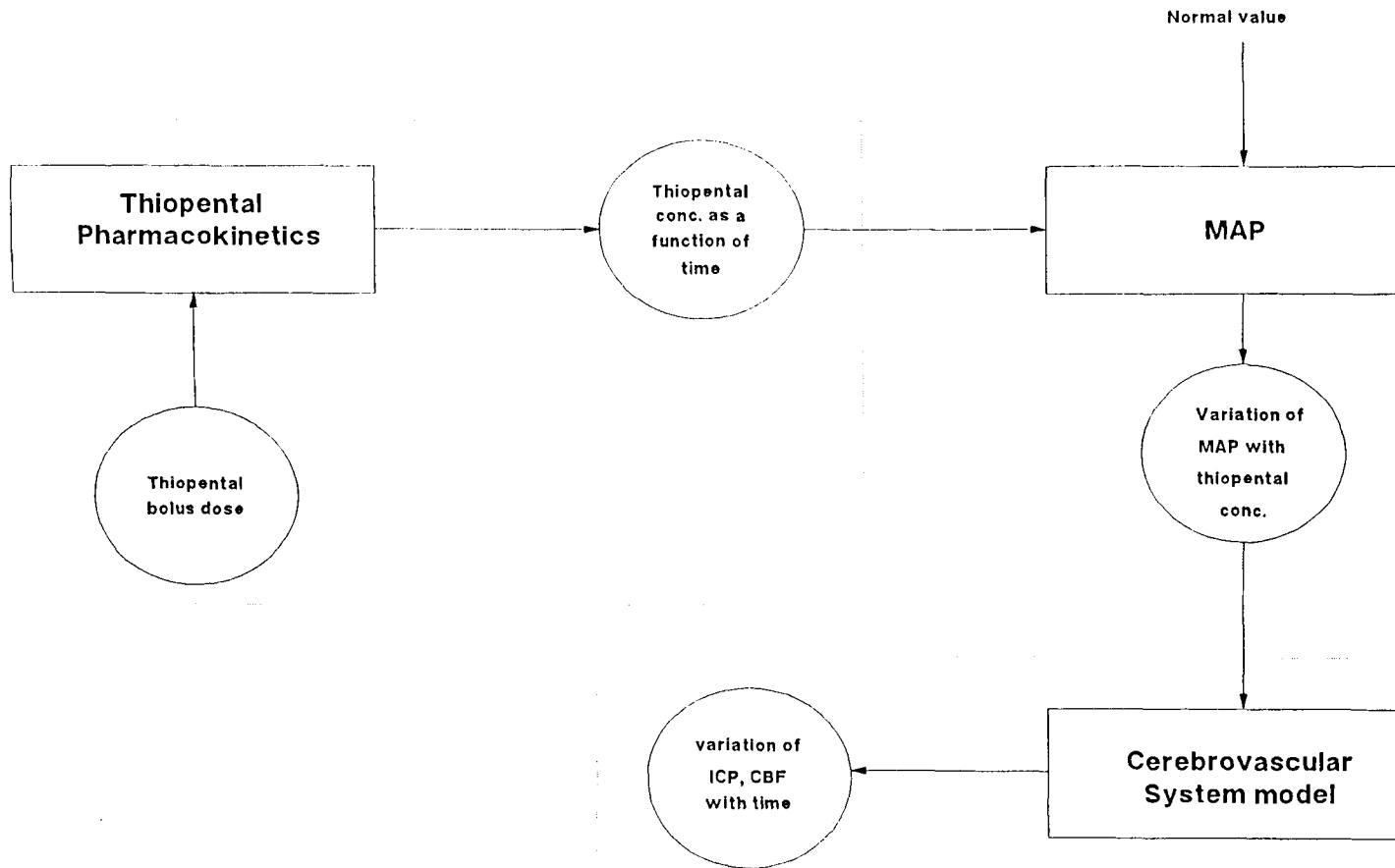


Fig. 2.12. Interrelationship Between Thiopental Pharmacokinetics and Cerebrovascular System

used to calculate the effect of thiopental on MAP and arterial resistance. The TUTSIM block diagrams for these are shown in fig 2.10 and 2.11. Figure 2.12 is a schematic diagram which shows the interactions between the Thiopental Pharmacokinetic model and the ICP simulation model.

### **2.3 Induction**

Having implemented the system using TUTSIM, the model is now ready for simulating the induction phase of anesthesia. Induction phase is defined as that phase of anesthesia which makes the patient unresponsive to surgical stimuli. This process is simulated by giving a bolus dose of thiopental, and then simulating the intubation process by increasing the MAP by about 45 mm Hg, after a time interval of two minutes. The results of this simulation are discussed in the next chapter.

## CHAPTER 3

### RESULTS

#### 3.1 Simulation of Induction Process

Simulation of induction process at various initial ICP is shown in figures 3.1-3.10. A bolus dose of thiopental is followed by laryngoscopy and intubation which increase mean arterial pressure from 95 mmHg to 140 mmHg.

Fig 3.1 shows the simulation at normal ICP. Initially the ICP is at 9.79 mm Hg. At  $t = 60$  sec, a bolus dose of 5mg/kg of thiopental is given. This causes the ICP to fall to about 8.52 mm Hg, i.e by 11.36%. It remains nearly at the same value until  $t = 180$  secs. Here MAP is increased from 95 to 140 mm Hg(intubation). This causes the ICP to rise to 11.9 mm Hg, which is higher than the initial value by 12.4%. ICP decreases slowly until  $t = 240$  sec, and then when MAP starts falling, ICP also falls and finally settles at 9.03 mmHg.

The same simulation is repeated for an initial ICP of 23.7 mm Hg (fig 3.2). Administration of thiopental causes ICP to fall to 20.28 mm Hg (11.83%). ICP then rises slowly due to autoregulatory mechanisms. At intubation, ICP acutely increases to 34.47 mm Hg, which is greater than the initial value by 17.39%, and settles around 32 mm Hg. Then, when MAP starts decreasing ( $t = 240$  sec), ICP falls off rapidly and becomes constant at 23.2 mm Hg.

Figure 3.3 shows a simulation at an initial ICP value of 32 mm Hg. Here thiopental causes ICP to fall by 5 mm Hg (15.63%). An increase in MAP causes ICP to rise to 39.4 mm Hg (12.5%), and then finally settle at about 33 mm Hg 300 seconds. Fig 3.4 shows the simulation at an ICP of 38mm Hg. Here Thiopental administration causes ICP to fall by about 4 mm Hg (15.79%) and intubation causes ICP to rise by 11.5 mm Hg (18.42%). Then ICP falls off gradually, as seen



in figure 3.3, and settles at about 39 mm Hg. Similar results are seen in fig 3.5 for an initial ICP of 50 mm Hg.

Thus computer simulation predicts 11 to 16 % reduction in ICP following injection of a thiopental bolus of 5mg/kg, and the reduction increases as the initial value of ICP increases. However, rapid redistribution of thiopental limits the duration of this effect to about 2.5 minutes. Subsequent laryngoscopy and intubation, which is associated with an increase in MAP of 45 mm Hg, causes acute intracranial hypertension, exceeding the initial ICP by 11 to 19% depending on the initial ICP - the higher the ICP, the greater the increase. To minimize this deviation a second dose of thiopental is injected just before intubation. Figures 3.6 to 3.10 shows these simulations various ICPs. In fig 3.6, it is observed that a second dose of thiopental (3mg/kg) causes ICP to decrease to about 8.3 mm Hg. Intubation causes ICP to rise to 9.38 mm Hg. This increase is smaller than that obtained in fig 3.1 without the second dose of Thiopental . Thus the additional dosage helps to maintain the ICP closer to its normal value during intubation. In fig 3.7 the maximum value of ICP is 29 mm Hg as against 32 in fig 3.2, for the same initial value of ICP. Similarly in simulations shown in fig 3.8, 3.9 and 3.10 the peak ICP observed was 35.7 mm Hg, 46 mm Hg and 56 mm Hg as compared with 39.5, 49.7, 59.6 mm Hg respectively for the same initial ICP. These simulations suggest that administering a second dose of Thiopental just before intubation can keep the ICP closer to control values than just a single dose of Thiopental administered earlier.

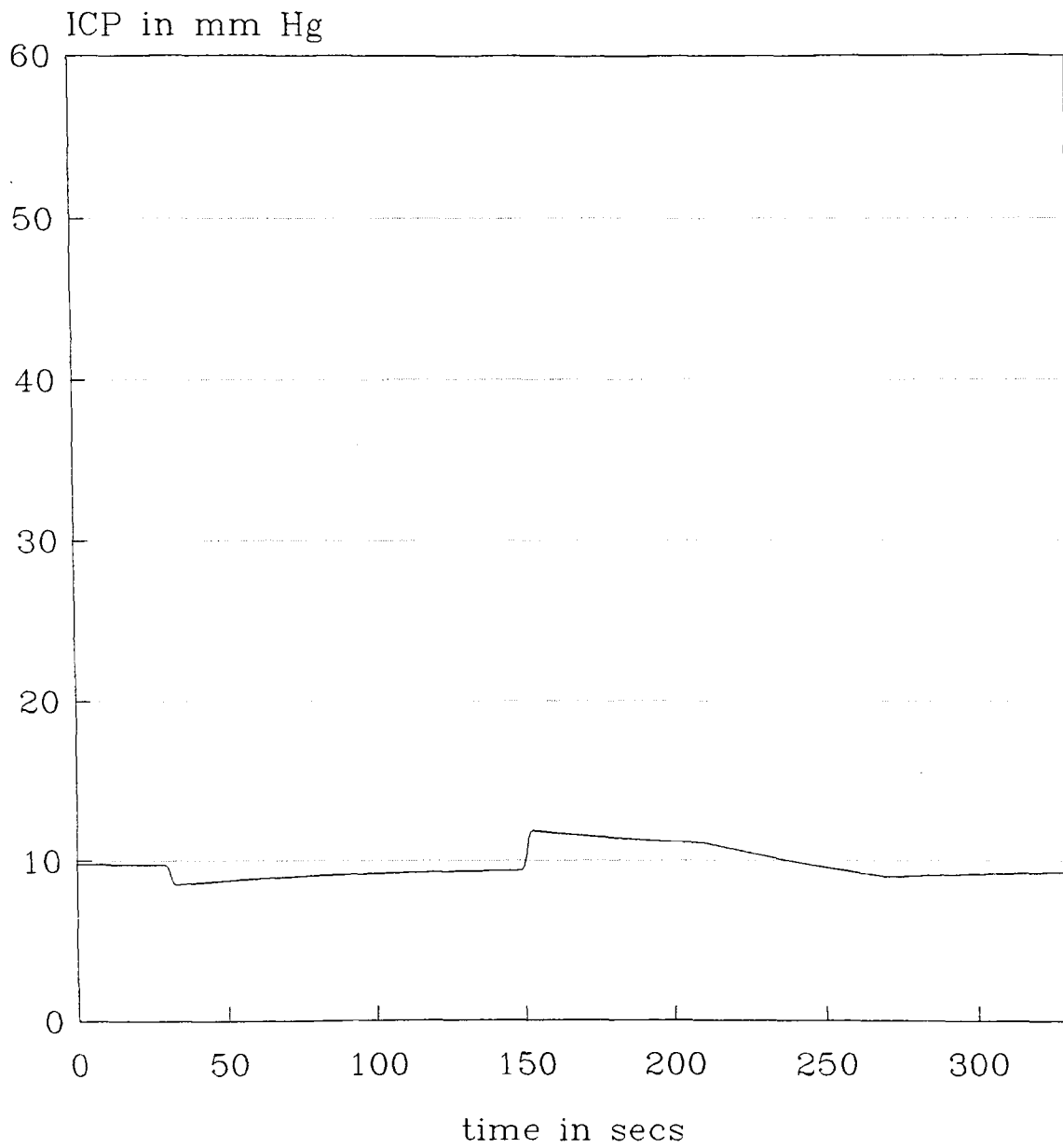


Fig. 3.1 ICP vs Time, Initial ICP=9.7mmHg

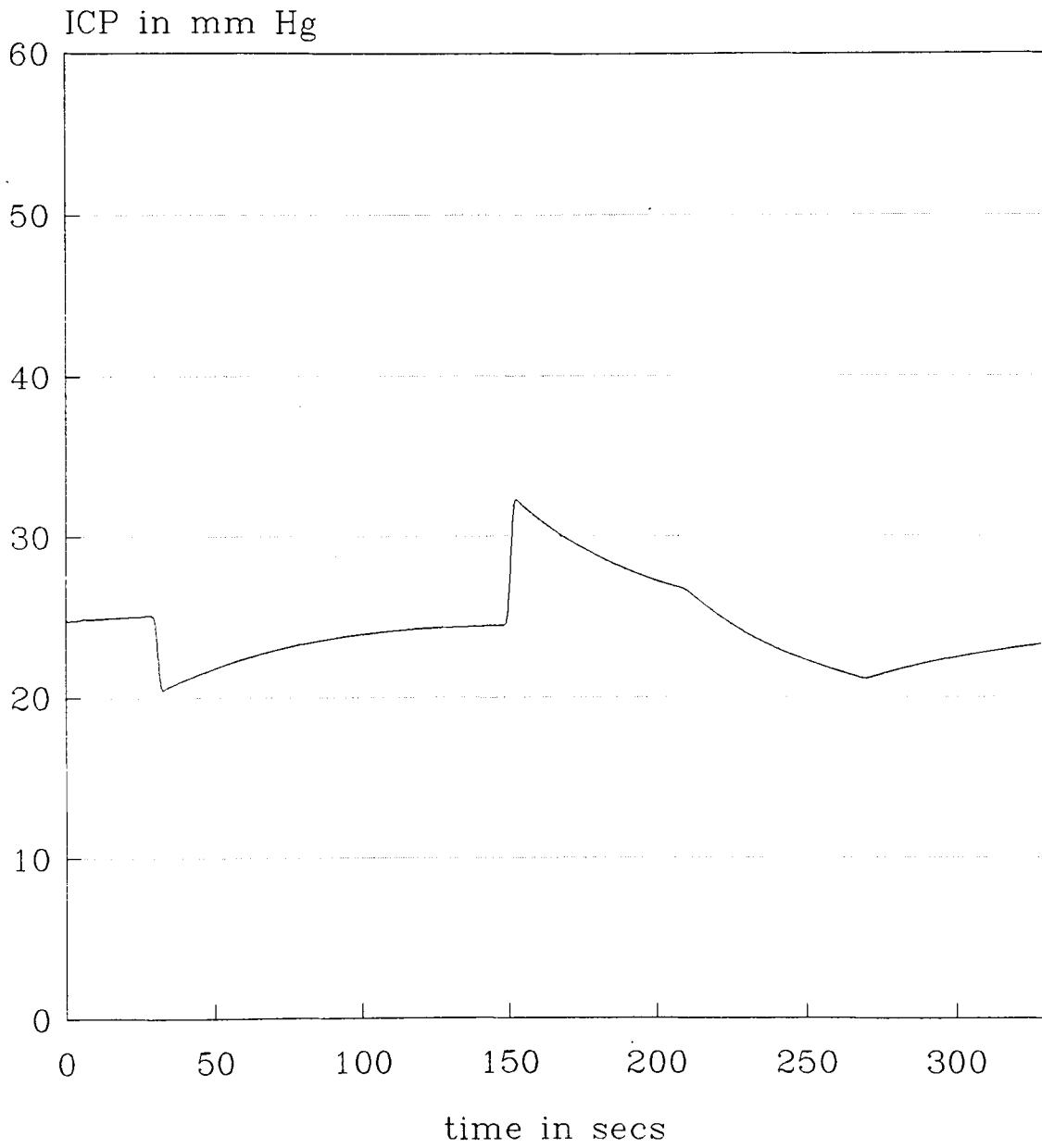


Fig. 3.2 ICP vs Time, Initial ICP=24mmHg

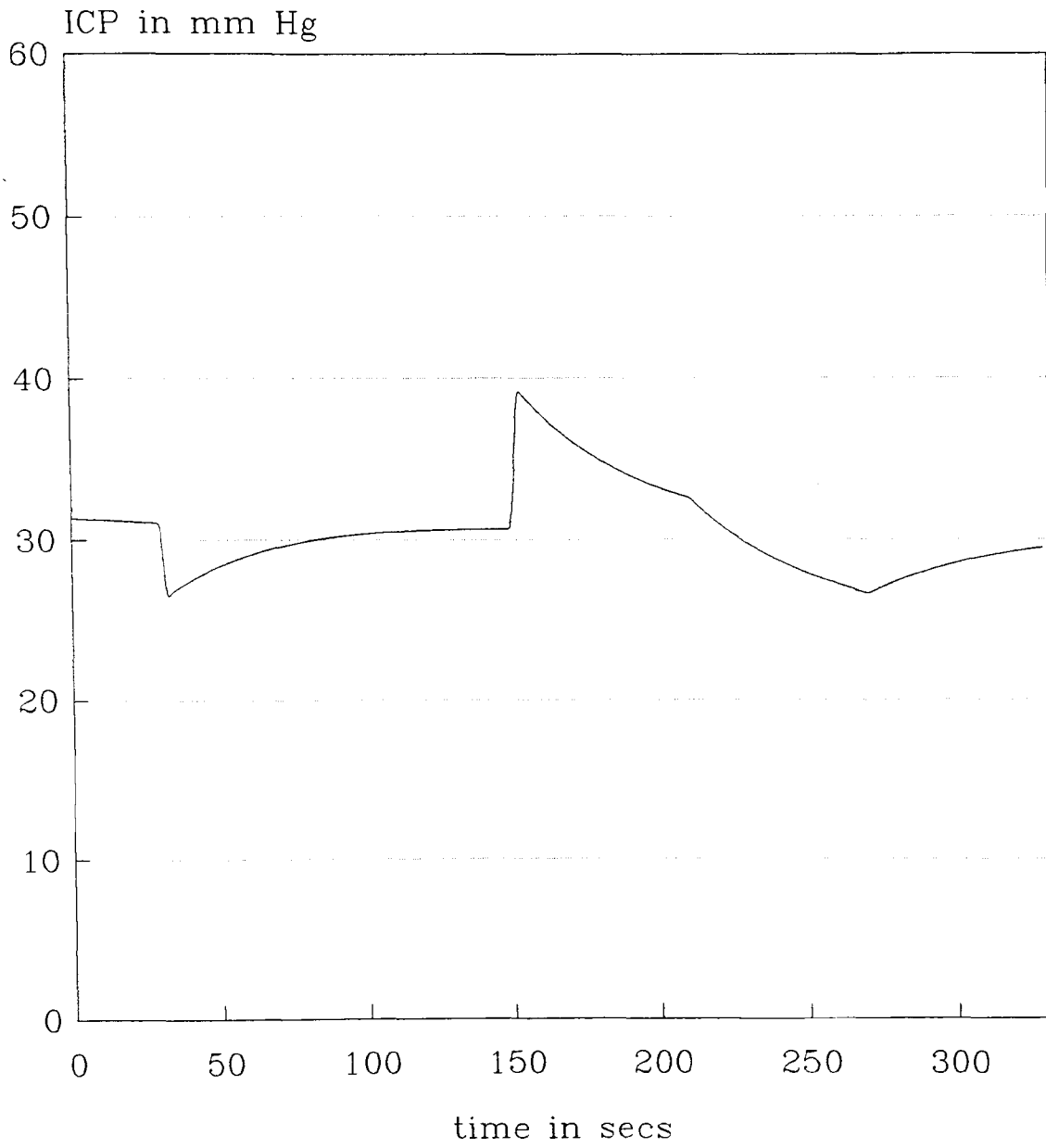


Fig. 3.3 ICP vs Time, Initial ICP=32mmHg

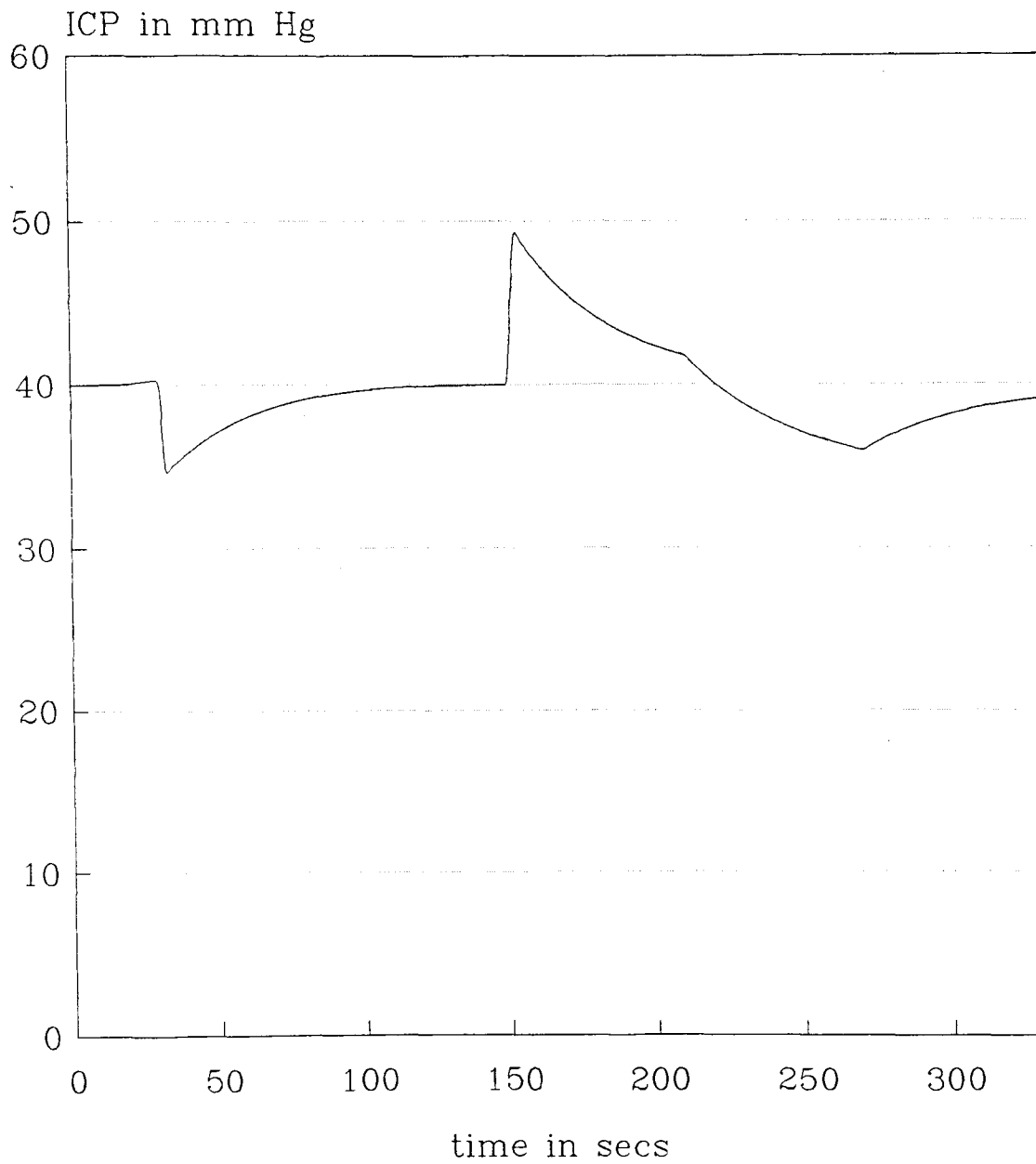


Fig. 3.4 ICP vs Time, Initial ICP=40mmHg

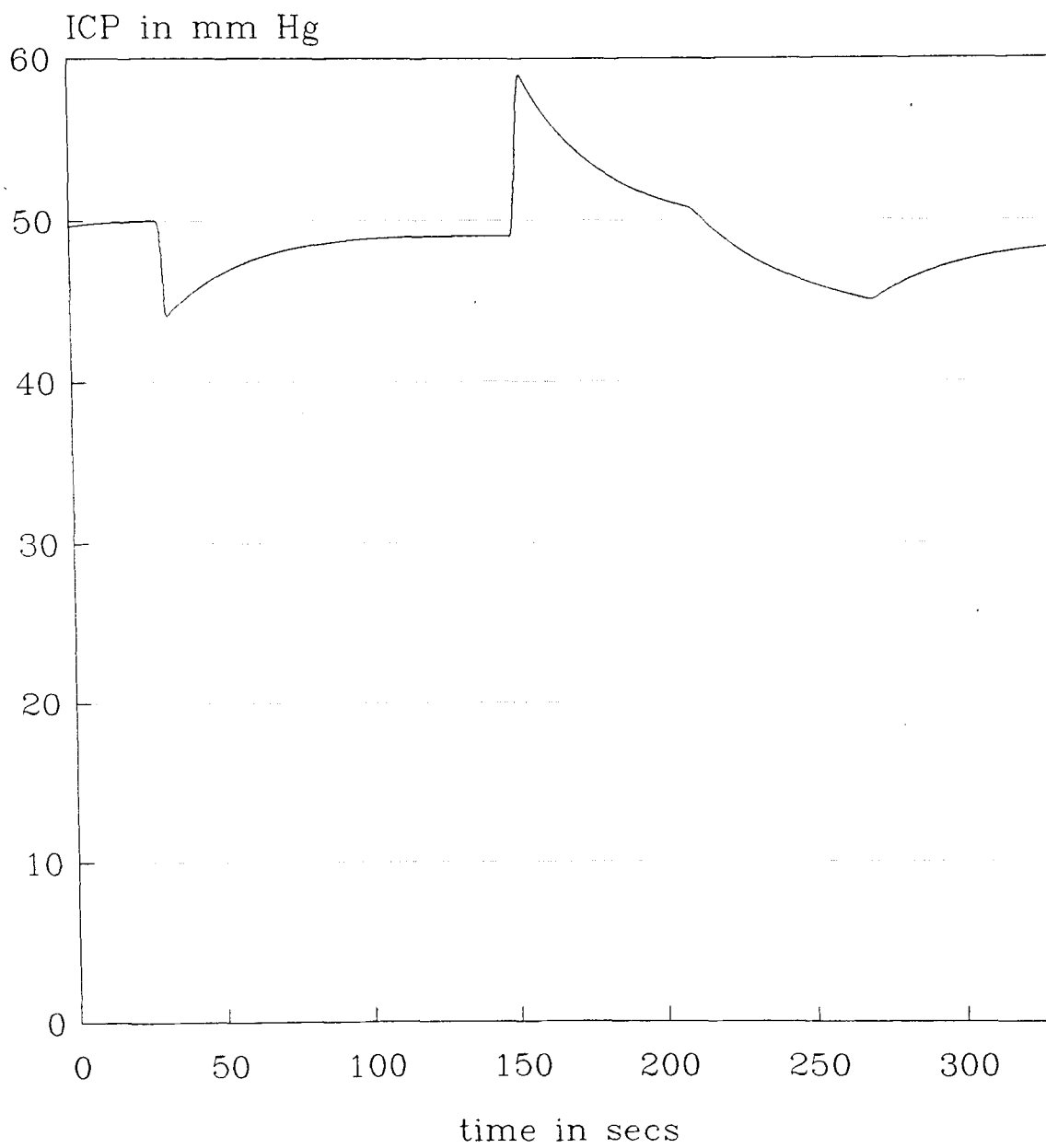


Fig. 3.5 ICP vs Time, Initial ICP=50mmHg

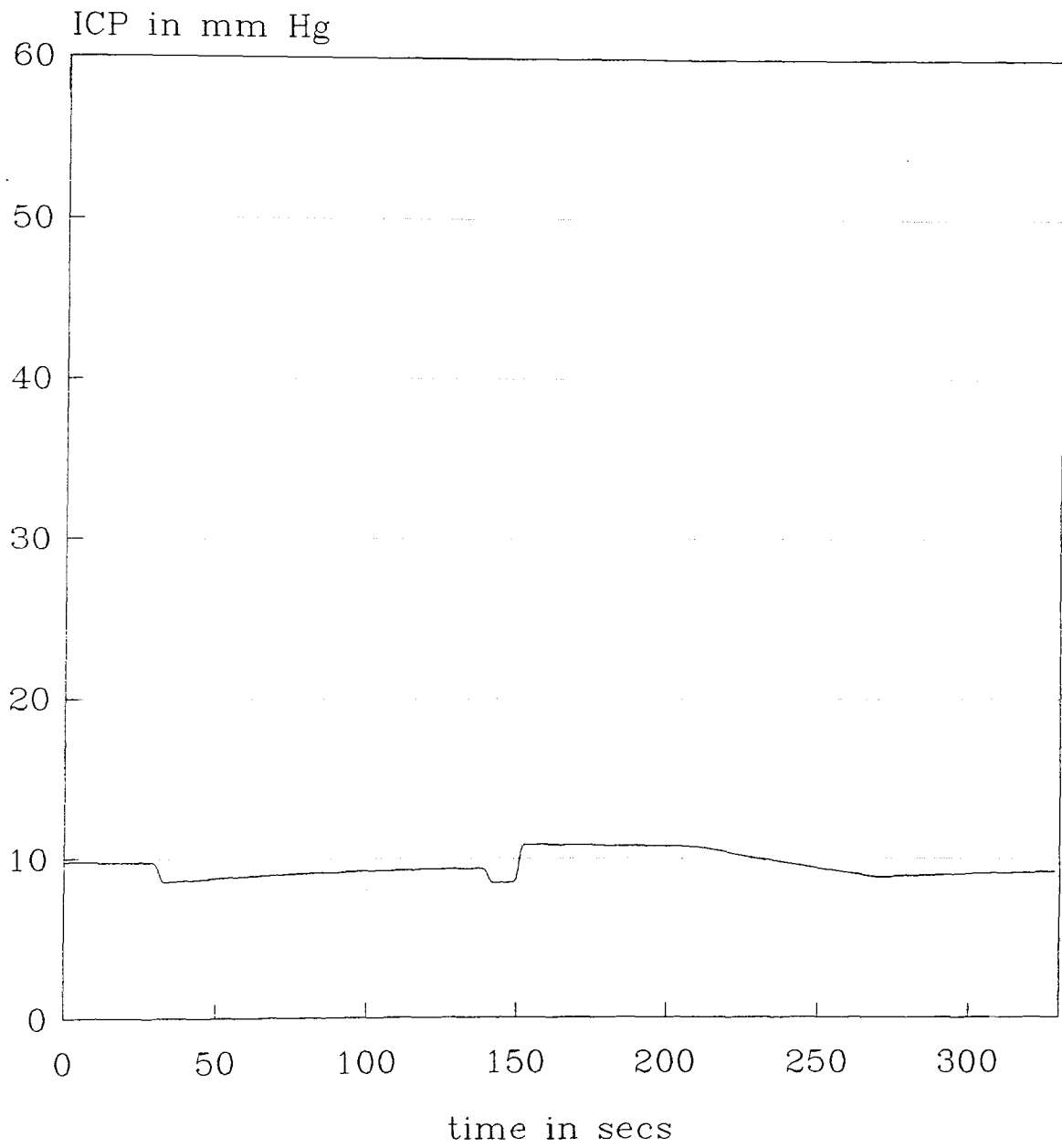


Fig. 3.6 ICP vs Time, Initial ICP=9.7mmHg

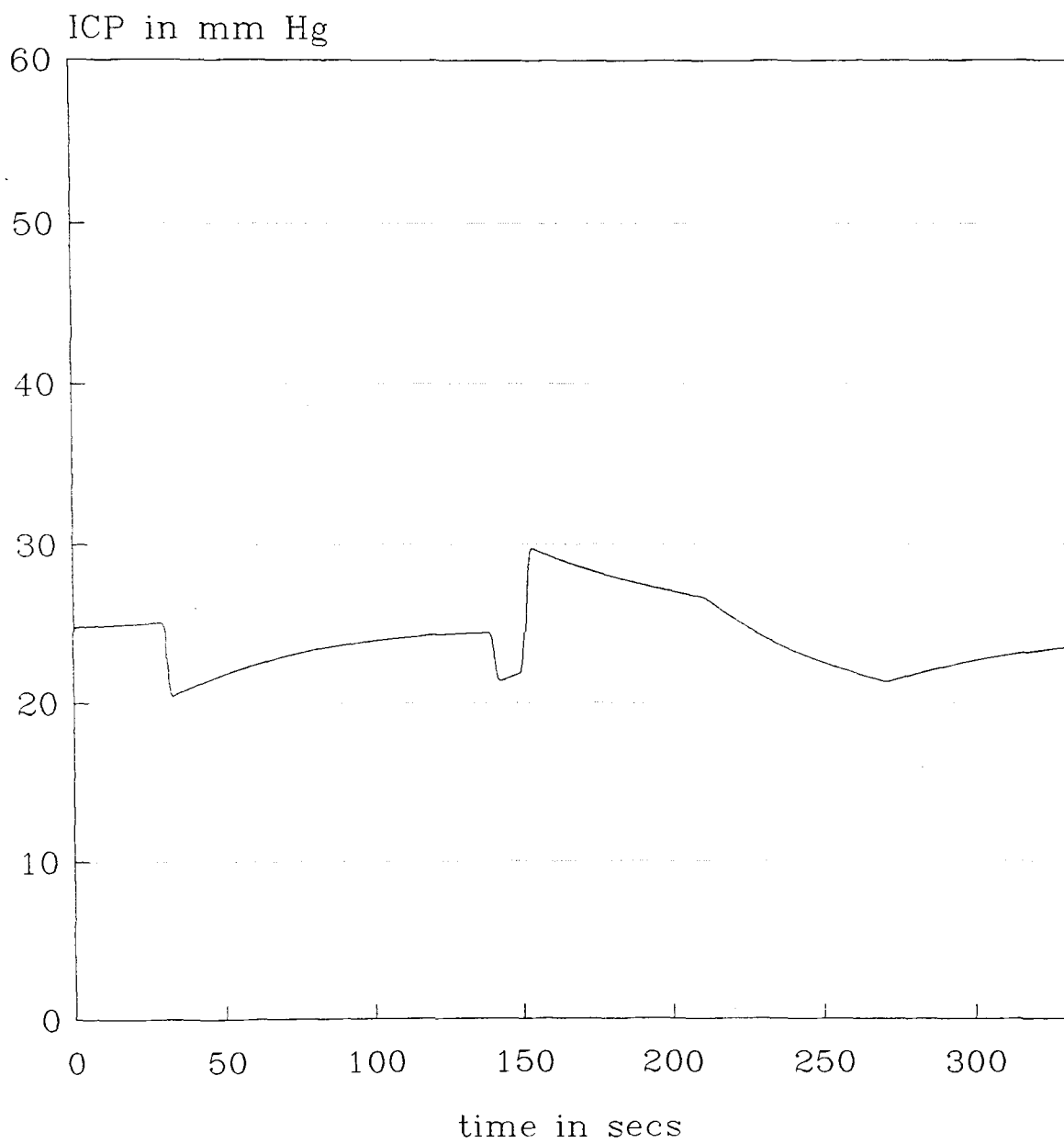


Fig. 3.7 ICP vs Time, Initial ICP=24mmHg



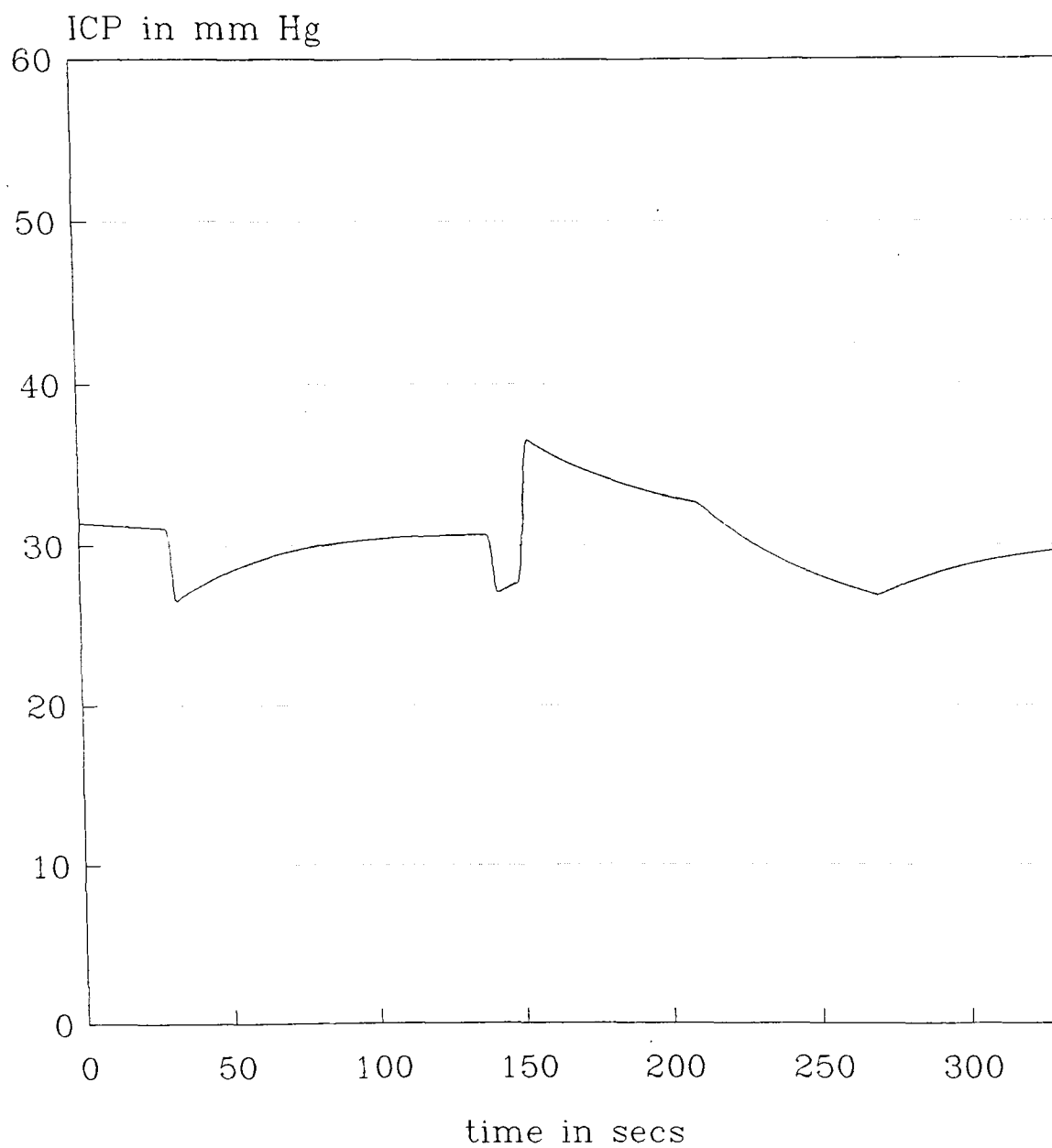


Fig. 3.8 ICP vs Time, Initial ICP=32mHg

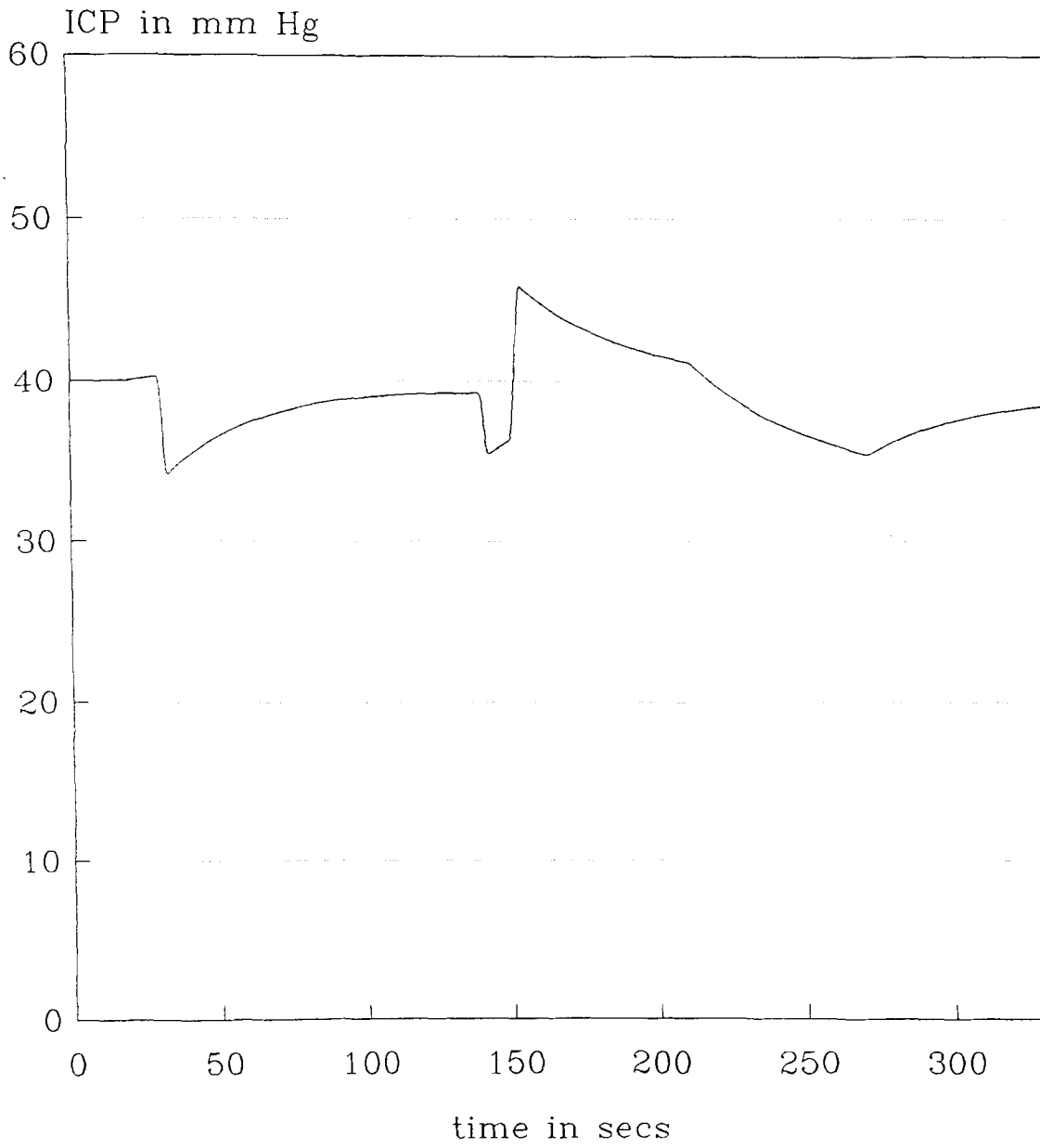


Fig. 3.9 ICP vs Time, Initial ICP=40mHg

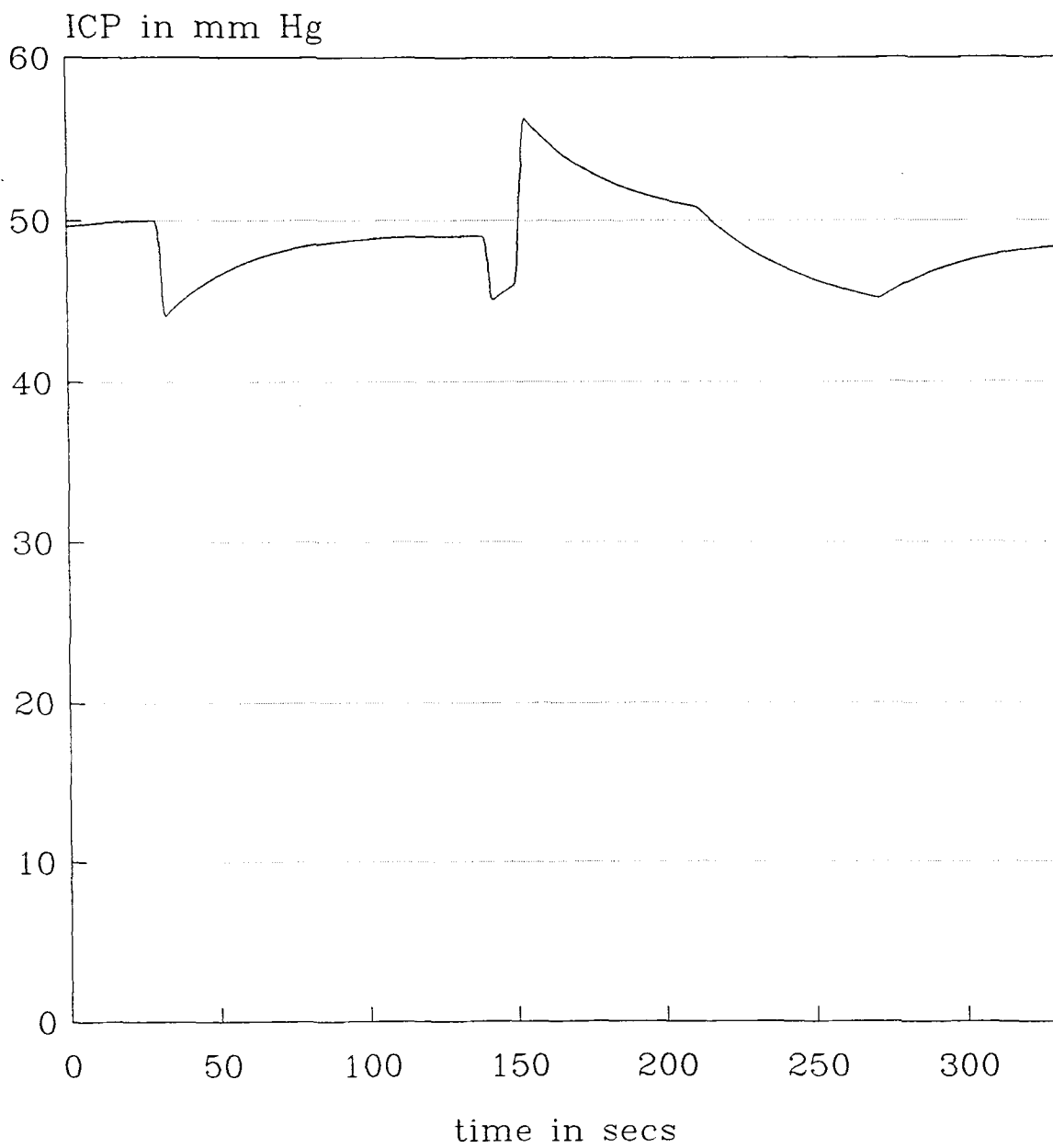


Fig. 3.10 ICP vs Time, Initial ICP=50mHg

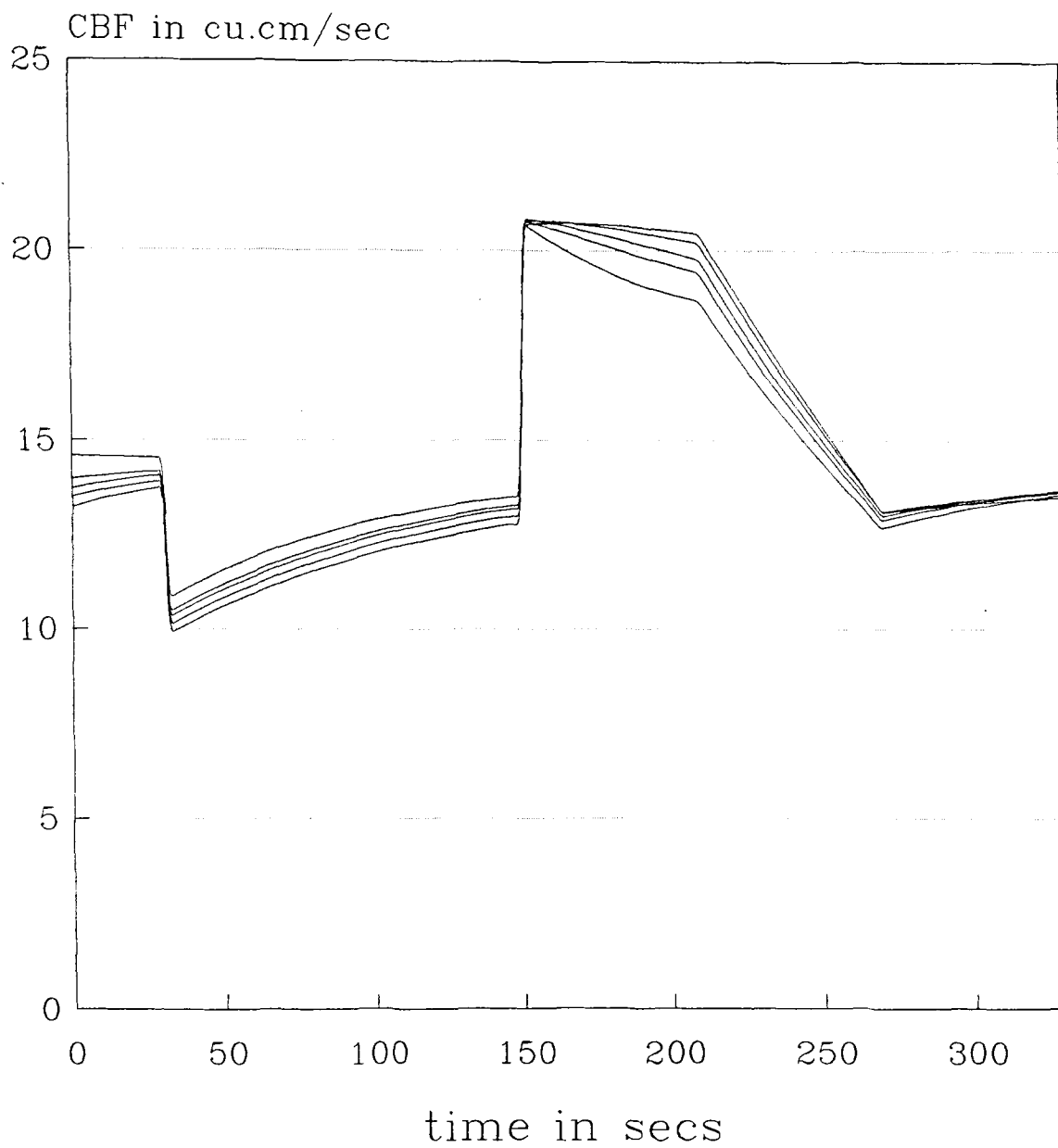


Fig. 3.11 CBF vs Time, Single Dose

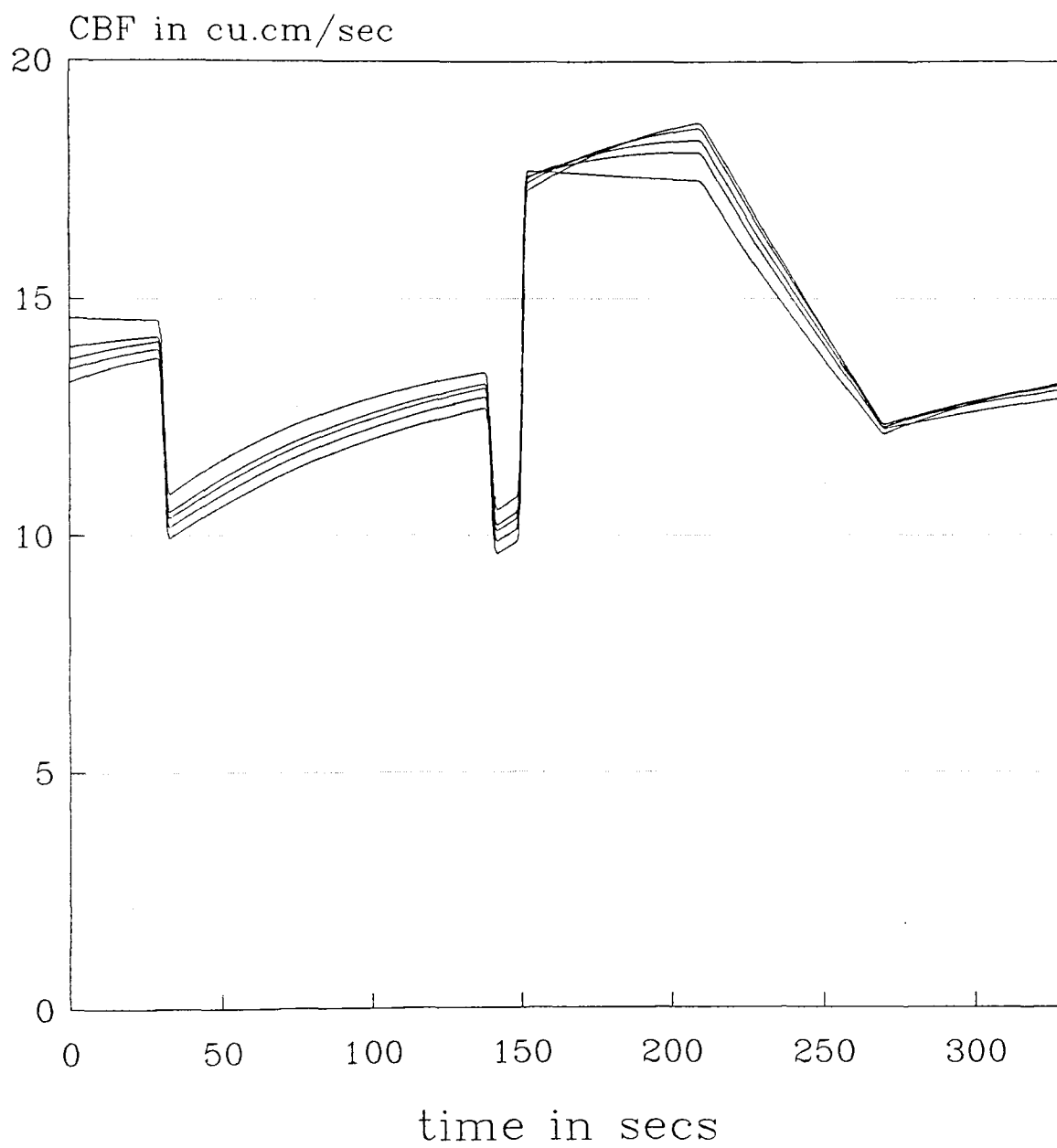


Fig. 3.12 CBF vs Time, Double Dose

## CHAPTER 4

### DISCUSSION

There have been several studies in recent years which attempt to clarify the origin and clinical significance of ICP dynamics. Most of these studies were experimental, providing interesting data both on man and animals. A few mathematical models of overall intracranial hemodynamics have also been proposed in order to quantitatively describe the CSF pressure and volume changes in several clinical and experimental conditions. However, most authors who developed mathematical models for intracranial hemodynamics focussed their attention only on a particular aspect of it, such as the CSF pressure volume relationship (2), CSF production and absorption kinetics (3,4) or the collapsibility of the cerebral venous vascular bed(1,6).

In our study, an original mathematical model of the overall human intracranial hemodynamics is proposed which elucidates the role of different factors in determining the time pattern of intracranial pressure. Both the arterial and the venous, as well as the tissue compartments and the CSF production and absorption mechanisms were separately examined from a mathematical point of view and included in the model. Autoregulatory adjustments of arterial-arteriolar resistance in order to change flow towards its control value were also introduced. In addition to these, effect of drugs (thiopental) on the arterial resistance and mean arterial pressure, and hence on ICP were also introduced.

The main original contribution of the present model is its ability to take a great number of different features of intracranial dynamics simultaneously into account. To our knowledge this characteristic is unique, since no model proposed in the past has been able to combine so many properties of cerebral hemodynamics.

The importance of having combined many aspects of intracranial dynamics is especially important at high values of ICP. In fact, in this condition, intracranial dynamics is the result of many causes like increases in venous pressure due to venous collapse, increases in arterial pressure, stiffening of the intracranial compartment, progressive loss of autoregulation, changes in CSF production and absorption rates ; all of these aspects should be simultaneously taken into account if correct a description of the phenomenon under study is to be presented.

#### **4.1 Assumptions**

A model is a representation of a complex system. The essence of creating a model is to capture the properties of the system, yet keep the model simple enough to conceptualize. Therefore, models are built on a set of simplifying assumptions. The strength of the model depends on the strengths of its assumptions.

The major assumptions of the proposed model are

1. Resistances and compliances are lumped in the boundary between the compartments.
2. Resistances relate fluid flux to gradient and compliances relates fluid accumulation to rate of pressure change.
3. An Exponential relationship between thiopental concentration and arterial resistance.

#### **4.2 Critique**

The major shortcomings of the model are

1. The metabolic factors affecting the cerebrovascular system were not considered.

2. The model developed is a simple pharmacokinetic distribution model coupled with a simple compartmental model of the normal physiology of ICP. No pathological conditions were considered.
3. Chemical factors affecting the arterial pressure, like concentration of oxygen and carbon dioxide were not taken into account.

### 4.3 Interpretation

The time interval between injection of thiopental and intubation depends on the type of neuromuscular relaxant. In case of a depolarizing neuromuscular relaxant (eg. succinyl choline) the time interval is about 1 minute. In the case of a non depolarizing neuromuscular relaxant (eg. vecuroisine), this time is roughly about 2.5 minutes. In our study it was assumed that non-depolarizing agents were used and hence the time interval between drug injection and intubation was taken as 2 minutes.

Computer simulation predicts that thiopental in bolus doses (5 mg/kg) significantly reduces the ICP by about 11 to 16 % . This effect was present for only about 2.5 minutes due to the rapid redistribution of thiopental. The effect was minimum in the case of normal ICP (ICP < 10 mm Hg), and increased as ICP increases. Fig 3.19 to 3.20 shows the efficacy of thiopental in reducing abnormally elevated ICP.

Intubation causes ICP to exceed its initial value by 11 to 19 % . The increase was found to be greater in those cases where the initial ICP values were above normal. Administration of a second dose of thiopental just before intubation reduces the increase in ICP due to intubation by nearly 10 % . This finding suggests that injecting a second dose of the drug (perhaps of lesser strength) can be used as a technique to keep ICP closer to control values during the induction phase of anesthesia.



#### **4.4 Conclusion**

Computer simulation and modeling suggests that multiple doses of drug may be able to control ICP during various phases of anesthesia than a single dose of drug administered at an earlier time. It was demonstrated that if the time interval between the administration of a drug and intubation is more than two minutes, then an additional dose of thiopental is required to prevent an elevation in ICP during laryngoscopy. Results of simulations such as the one in the study may lead to more optimal strategies for regulating ICP during the various phases of anesthesia.

## **APPENDIX**

The appendix contains a listing of the TUTSIM code for the Cerebrovascular System Model developed.



				P1=	1.0000
37	FNC	36			
X,Y-	1	0.0000	75.0000		
X,Y-	2	0.1500000	125.0000		
X,Y-	3	0.3500000	95.0000		
X,Y-	4	0.5000000	105.0000		
X,Y-	5	0.8000000	75.0000		
38	LIM	37		P1=	999.990E+03
				P2=	0.0000
39	FND	34		P1=	40.0000
40	FNC	36			
X,Y-	1	0.0000	75.0000		
X,Y-	2	0.1500000	125.0000		
X,Y-	3	0.3500000	95.0000		
X,Y-	4	0.5000000	105.0000		
X,Y-	5	0.8000000	75.0000		
41	DIF	700		P1=	0.0000
				P2=	0.0000
42	GAI	41		P1=	0.0030000
50	HIS	23		P1=	0.0000
51	ATT	2		P1=	526.0000
60	CON			P1=	1.0000
61	SUM	700	-3		
62	GAI	61		P1=	3.6800
63	DIV	60	62		
64	SUM	1	-2		
65	SUM	1	-3		
66	DIV	64	65		
67	GAI	66		P1=	0.3600000
68	CON			P1=	-2.5000
69	SUM	-68	65		
70	GAI	69		P1=	0.3100000
71	DIV	60	70		
72	CON			P1=	7.5000
73	DIV	603	72		
74	MUL	73	73		
75	SUM	74	3		
76	GAI	75		P1=	0.2000000
77	DIV	60	76		
78	SUM	63	71	77	
104	DIV	4	67		

108	DIV	8	67		
120	INT	128			
				P1=	0.0000
121	CON				
				P1=	95.0000
122	CON				
				P1=	15.0000
123	SUM	-121	122	700	-1
124	SUM	121	122		
125	DIV	123	124		
126	ATT	125			
				P1=	60.0000
127	ATT	120			
				P1=	-60.0000
128	SUM	126	127		
129	CON				
				P1=	3.1400
130	ATN	140			
131	DIV	130	129		
132	SUM	60	-131		
133	ATT	132			
				P1=	3.0000
140	MUL	129	120		
150	INT	155			
				P1=	0.0000
151	CON				
				P1=	13.6700
152	ATT	150			
				P1=	-60.0000
153	SUM	151	-680		
154	ATT	153			
				P1=	60.0000
155	SUM	154	152		
156	MUL	152	129		
157	ATN	156			
158	ATT	157			
				P1=	10.0000
159	SUM	60	-158		
160	DIV	159	173		
161	SUM	160	133		
162	MUL	133	160		
165	DIV	162	161		
170	GAI	684			
				P1=	0.0367000
171	EXP	170			
172	SUM	171	-60		
173	GAI	171			
				P1=	3.0000
255	PLS				
				P1=	20.0000
				P2=	1.000E+03
				P3=	0.0380000
260	PLS				
				P1=	10.0000

				P2=	11.0000
				P3=	6.0000
261	SUM	170	260		
300	TIM				
301	GAI	300			
				P1=	1.2500
302	FIX	301			
303	GAI	301	-302		
				P1=	0.8000000
304	FND	303			
				P1=	306.0000
305	GAI	300			
				P1=	1.0000
306	FNC	305			
X, Y-	1	0.0000	14.0385		
X, Y-	2	0.2400000	17.1668		
X, Y-	3	0.4300000	16.0166		
X, Y-	4	0.5300000	16.0000		
X, Y-	5	0.8000000	14.0385		
307	LIM	306			
				P1=	999.980E+03
				P2=	0.0000
308	FND	303			
				P1=	309.0000
309	FNC	305			
X, Y-	1	0.0000	75.0000		
X, Y-	2	0.3000000	125.0000		
X, Y-	3	0.4000000	95.0000		
X, Y-	4	0.5000000	105.0000		
X, Y-	5	0.8000000	75.0000		
400	CON				
				P1=	526.3160
401	CON				
				P1=	0.1600000
402	MUL	400	401		
403	SUM	400	401		
404	DIV	402	403		
405	CON				
				P1=	0.8803000
406	CON				
				P1=	0.3610000
407	SUM	404	405	406	
408	CON				
				P1=	2.3810
409	MUL	407	408		
410	SUM	407	408		
411	DIV	409	410		
412	SUM	411	165		
413	DIV	60	165		
601	LIM	1			
				P1=	0.0000
				P2=	30.0000
602	LIM	2			
				P1=	0.0000

603	LIM	3							P2=	6.0000
									P1=	0.0000
									P2=	25.0000
679	SUM	700	-2							
680	DIV	679	413							
681	GAI	680								
									P1=	1.6625
684	INT	694							P1=	0.0000
685	INT	695							P1=	0.0000
686	INT	696							P1=	0.0000
687	GAI	684							P1=	0.0000
688	GAI	685							P1=	-0.0098500
689	GAI	686							P1=	0.0013120
690	GAI	685							P1=	64.800E-06
691	GAI	684							P1=	-0.0013200
692	GAI	686							P1=	0.0080000
693	GAI	684							P1=	64.800E-06
									P1=	0.0017830
694	SUM	687	688	689	711	800	797			
695	SUM	690	691							
696	SUM	692	693							
697	PLS									
									P1=	60.0000
									P2=	61.0000
									P3=	345.6250
698	CON								P1=	95.0000
699	GAI	684							P1=	3.3200
700	SUM	698	-699	801	807					
710	ATT	697								
									P1=	5.5300
711	GAI	710							P1=	0.0800000
784	GAI	684							P1=	12.5000
797	PLS									
									P1=	0.0000
									P2=	0.0000
									P3=	0.0000
800	CON								P1=	0.0000
801	PLS								P1=	0.0000

				P2= 180.0000
				P3= -45.0000
802	CON			
				P1= 900.0000
803	TIM			
804	GAI	803		
				P1= 3.0000
805	SUM	802	-804	
806	ATT	805		
				P1= 4.0000
807	LIM	806		
				P1= 0.0000
				P2= 45.0000



## REFERENCES

1. Shaul Soreh, Jacob Bear and Zvi Karni: "Resistances and Compliances of a Compartmental Model of the Cerebrovascular System". *Annals of Biomedical Engineering* 17: 1-12, 1989.
2. Alim Louis Benabid, Jaques de Raugement, Michel Barge: "CSF Dynamics - A mathematical model". *Intracranial Pressure, Volume 1*, 1971.
3. Bernhard Hoffernath, Frank Matakao, Emanuel Fretschka: "A Computer model of CSF Dynamics". *Intracranial Pressure, Volume 4*, 1974.
4. Oscar Hoffman: "Biomathematics of Intracranial CSF and Hemodynamics, Simulation and Analysis with the aid of mathematical model". *Acta Neurochirurgica, supplementary 40*: 117-130, 1987.
5. Takemae, Kosugi, Ihebe, Kumagai, Matsuyama: "A simulation study of ICP increment using Electrical Circuit model of Cerebral Circulation". *IEEE Transactions on Biomedical Engineering* 34: 958-962, 1987.
6. Marmarou, Shulman, Rosende: "Non linear analysis of the Cerebrospinal fluid system and Intracranial Pressure". *Journal of Neurosurgery* 48: 332-344, 1978.
7. Giammarco, Ursino, Belardinelli: "A mathematical model of Cerebral blood flow Chemical Regulation". *IEEE Transactions on biomedical engineering* 36: 183-191, 1989.
8. Mauro Ursino: "A mathematical study of Human Intracranial Hemodynamics. Part I - The cerebrospinal fluid pressure". *Annals of Biomedical Engineering* 16: 379-397, 1988.
9. Elizabeth M. Wagner and Richard J. Traystman: "Cerebrovascular Transmural Pressure and Autoregulation". *Annals of Biomedical Engineering* 13: 311-320, 1985.
10. Harper, Bohlen, Rubin: "Arterial and Microvascular Contributions to Cerebral Cortical Autoregulation in Rats". *Annals of Biomedical Engineering* 18: 379-387, 1989.
11. L. Baumbach, D. Heistad: "Regional, Segmental and Temporal Heterogeneity of Cerebral Vascular Autoregulation". *Annals of Biomedical Engineering* 13: 303-310, 1985.
12. H.A. Kontos, E.P. Wei, R.M. Navari: Responses of Cerebral Arteries and Arterioles to Acute Hypotension and Hypertension". *Am. J. Physiol* 234: H371-H383, 1978.
13. M.M. Ghoneim and M.J. Van Hamme: "Pharmacokinetics of Thiopentone-Effects of Enflurane and Nitrous oxide". *Br. J. Anesth.*: 1237-1242, 1978.
14. H.M. Shapiro, A. Gilando, S.R. Wyte & A.B. Harris: "Rapid Intraoperative Reduction of Intracranial Pressure with Thiopentone". *Br. J. Anesth.*: 1057-1061, 1973.

15. H. Stullken, H. Milde, D. Michenfelder, H. Tinker: "The nonlinear responses of Cerebral Metabolism to Low Concentration of Halothane, Enflurane, Isoflurane and Thiopental". *Anesthesiology* 46: 28-34, 1977.
16. Ellen B. Rudy, Mara Baun, Kathleen Stone, Barbara Turner: "The Relationship Between Endotracheal Suctioning and Changes in Intracranial Pressure: A Review of Literature". *Suctioning and Intracranial Pressure* 15: 488-494, 1986.
17. Donald Stanski, Pierre O. Maitre: "Population Pharmacokinetics and Pharmacodynamics of Thiopental-The effect of Age Revisited". *Anesthesiology* 72: 412-422, 1990.
18. Elizabeth J. Fox, Garry Sklar, H. Hill, D. King: "Complications Related to the Pressor Response to Endotracheal Intubation". *Anesthesiology* 47: 524-525, 1977.
19. E. Moss, D. Powell, R.M. Gibson and D.G. McDowall: "Effects of Tracheal Intubation on Intracranial Pressure following Induction of Anesthesia with Thiopentone or Althesin in patients undergoing neurosurgery". *Br. J. Anesth.* 50: 353-359, 1978.
20. A. Schwid, W. Buffington, P. Strum: "Computer Simulation of the Hemodynamic Determinants of Myocardial Oxygen Supply and Demand". *Journal of Cardiothoracic Anesthesia* 4, No 1: 5-18, 1990.
21. Mauro Ursino and Patrizia Di Giammarco: "A mathematical model of the Relationship between Cerebral Blood Volume and Intracranial Pressure Changes-The Generation of Plateau Waves". *Annals of Biomedical Engineering* 19: 15-42, 1991.
22. H.M. Shapiro, S.R. Wyte, A.B. Harris, A. Galindo: "Acute Intraoperative Intracranial Hypertension in Neurosurgical Patients". *Anesthesiology* 37: 399-405, 1972.
23. Donald Martin, Henry Rosenberg, Stanley J. Aukburg, McIver Edwards: "Low-Dose Fentanyl Blunts Circulatory Responses to Tracheal Intubation". *Anesthesia and Analgesia* 61: 680-684, 1982.